Hydrogen molecule in a strong parallel magnetic field

Yu. P. Kravchenko and M. A. Liberman
Department of Physics, Uppsala University, Box 530, S-751 21, Uppsala, Sweden
and P. Kapitsa Institute for Physical Problems, Russian Academy of Sciences, 117334 Moscow, Russia
(Received 3 November 1997)

We investigate the hydrogen molecule in a strong parallel magnetic field using a fully numerical Hartree-Fock approach. We find that for magnetic fields below 4.2×10^4 T the ground state of H_2 is the strongly bound singlet state $^1\Sigma_g$, for magnetic fields stronger than 3×10^6 T the ground state of the molecule is the strongly bound triplet $^3\Pi_u$, and for magnetic fields between 4.2×10^4 T and 3×10^6 T the symmetry of the ground state is the triplet state $^3\Sigma_u$, which is characterized by repulsion at intermediate internuclear distances and by a weak quadrupole-quadrupole interaction between atoms at large internuclear separation. In this region of magnetic field strength the hydrogen molecule is bound weakly, if at all; the hydrogen atoms behave like a weakly nonideal gas of Bose particles and can form a superfluid phase predicted in earlier works [Korolev and Liberman, Phys. Rev. Lett. **72**, 270 (1994)]. For magnetic fields between $\approx3\times10^5$ T and 3×10^6 T the triplet state $^3\Pi_u$ is found to be metastable. This state may be responsible for an unknown excitonic line observed experimentally [Timofeev and Chernenko, JETP Lett. **61**, 617 (1995)]. [S1050-2947(98)01105-6]

PACS number(s): 33.15.Bh, 31.15.Ne, 71.35.−y, 95.30.Ft

I. INTRODUCTION

The intriguing world of atomic and molecular phenomena in strong magnetic fields, which was brought to the attention of investigators after the discovery of such fields on the surfaces of neutron stars [1] and white dwarfs [2], reveals a large number of unusual and spectacular effects. Serious attention to this area is motivated not only by pure theoretical interest, but also by practical applications in astrophysics and in the physics of semiconductors, where already laboratory magnetic fields become ''superstrong'' for excitons and shallow impurities.

The influence of a magnetic field H on the electron motion can be characterized by the energy distance $\hbar eH/m_ec$ between the Landau levels of the electron moving in that field. The magnetic field is ''strong'' on the atomic scale if this energy is comparable with the atomic unit of energy, i.e., 1 hartree. The two values become equal in the magnetic field $H_0=m_e^2e^3c/\hbar^3=2.350\,52\times10^9$ G, which is the atomic unit of magnetic field strength. The intensity of the magnetic field in atomic units may be conveniently defined as $\gamma=H/H_0$, and we shall use this designation throughout the paper. Magnetic fields in the atmospheres of white dwarfs are of the order of $\gamma\sim10^{-2}-5\times10^{-1}$ a.u., and fields on the surfaces of neutron stars and pulsars correspond to $\gamma\sim10^2-10^3$ a.u.

Magnetic fields of such magnitude dramatically modify the electronic structure of atoms and molecules. Electron spins tend to become antiparallel to the magnetic field, causing a complete restructuring of electronic shells, and electron clouds strongly contract in the direction perpendicular to the magnetic field. These effects are accompanied by the growth of binding energies of atoms and bonding energies between atoms in molecules. Because of the strong deformation of electronic orbitals, theoretical investigation of the electronic structure of matter in strong magnetic fields presents serious difficulties, and the well-developed computational techniques of ''field-free'' quantum chemistry usually require significant modifications.

Research inquiries in the area of strong magnetic fields are concentrated along several major lines of effort. One of them is the study of highly excited atomic and molecular states, the so-called Rydberg states, which can be observed experimentally in magnetic fields of the order of several tesla [3,4]. Another important direction of work focuses on the fundamental aspects of molecular and atomic structure in strong magnetic fields, primarily on the nuclear dynamics and nonadiabatic effects [5–8]. Finally, a significant deal of attention is paid to the calculations of the electronic structure of atoms, simple molecules, and condensed matter in magnetic fields.

Among the atoms, the most popular object of investigation is the hydrogen atom, which has been thoroughly studied both in the nonrelativistic [9] and relativistic approximations [10–12]. Detailed Hartree-Fock calculations have been performed for helium and heliumlike ions [13–15], including the negative ion H^- [16,17]. For atoms with more than two electrons, work has mostly been concentrated on the so-called adiabatic regime of superstrong magnetic fields, where both Hartree-Fock [18] and statistical models [19] were used. Recently, accurate Hartree-Fock calculations of many-electron atoms have been performed also for magnetic fields of intermediate strength [20].

The only molecule whose structure in the magnetic field is investigated in great detail is the one-electron hydrogen molecular ion H_2^+. The behavior of this system has been studied for both the parallel [21–23] and nonparallel configurations [24–26] with the aid of different approaches, including variational methods [21,24], basis set methods [22,25,26], and semianalytical approaches [23].

Among the molecules with more than one electron, the central place is occupied by the hydrogen molecule H_2. First of all, this is the simplest two-electron molecule, and it allows more detailed and accurate theoretical investigation than other molecules. Second, H_2 has a close solid-state analog, the excitonic molecule, which behavior in strong magnetic fields can be studied already in laboratory conditions.

The unit of ''strong'' magnetic field for the hydrogenlike excitons in direct-gap semiconductors is $H_0^{\rm eff}=m_{\rm eff}^2e^3c/\varepsilon^2\hbar^3$, where ε is the dielectric constant and $m_{\rm eff}$ is the reduced effective mass of the electron and the hole. For such semiconductors as Ge and InSb, $H_0^{\rm eff}$ can be less than 1 T, and the effects of strong magnetic fields on the excitonic spectrum can be observed in experiments [27].

However, the hydrogen molecule H_2 has been studied less thoroughly than H_2^+. If we turn to the problem of atomic hydrogen in a magnetic field, we will see that major computational difficulties always arose in the intermediate region of magnetic field strengths $\gamma\approx 1$ a.u. The same tendency holds for molecular hydrogen as well. Most of the publications dealing with H_2 in strong magnetic fields considered only the case of superstrong ($\gamma\sim 10^2-10^3$ a.u.) magnetic fields [28–30]. The behavior of H_2 in intermediate fields ($\gamma\sim 1$) attracted less attention and was mostly focused only on the triplet state $^3\Sigma_u$. Reference [31] reports finite basis set calculations of the term $^3\Sigma_u$ in a magnetic field $\gamma=1$ a.u. for parallel and perpendicular orientations of the magnetic field with respect to the molecular axis. The authors of [32] investigated the potential curve of $^3\Sigma_u$ at large internuclear separation and concluded that in strong magnetic fields $\gamma>1$ two atoms will form a molecule in the state $^3\Sigma_u$ due to van der Waals binding.

Because of the more complicated structure of the hydrogen molecule, even in superstrong magnetic fields $\gamma\gg 1$ the picture of its behavior remained unclear even qualitatively for a prolonged time. The assumption proposed in [28] was that the triplet state $^3\Sigma_u$ remains the ground state of the molecule even for superstrong magnetic fields $\gamma\gg 1$. In such a situation electron clouds of hydrogen atoms become strongly elongated in the direction of the magnetic field, and atoms acquire large quadrupole electric moments and may interact with each other by way of a quadrupole-quadrupole interaction. Since the magnitude of this interaction is rather small, atoms do not form strongly bound molecules: The molecules are bound very weakly, if at all, and hydrogen behaves like a nonideal gas of weakly interacting bosons. The thermodynamic properties of such a gas and possibility of Bose condensation of excitons in semiconductors in magnetic fields were investigated in [33].

However, later works [29,34] investigated another possibility, which was not explored previously: formation of the triplet state $^3\Pi_u$ in superstrong fields $\gamma\gg 1$. In the absence of a magnetic field, the state $^3\Pi_u$ is a short-lived state, because its potential curve lies above that of the states $^3\Sigma_u$ and $^1\Sigma_g$. However, Ref. [29] showed that in a strong parallel magnetic field the potential minimum of the state $^3\Pi_u$ becomes lower than the potential minimum of the state $^3\Sigma_u$, so that $^3\Pi_u$ becomes the ground state (all singlet states lie very high due to the contribution from electron spins), and the molecule will be strongly bound. This means that the theory of the Bose condensation of hydrogenlike gas in a magnetic field could be based on an incorrect assumption of the symmetry of the ground state [34].

Although the weakly interacting triplet state $^3\Sigma_u$ is not the ground state of the hydrogen molecule neither for small nor for very strong magnetic fields, one can see that it must be the ground state of H_2 in the intermediate region $\gamma\approx 1$ a.u. Let us compare the energies of the potential minima of all three state $^1\Sigma_g$, $^3\Sigma_u$, and $^3\Pi_u$. Since the state $^3\Sigma_u$ is characterized by repulsion at small and intermediate internuclear distances and by a weak interaction at $R\gg 1$ a.u., the minimum of the potential curve of the state $^3\Sigma_u$ almost coincides with the energy of two isolated hydrogen atoms in their ground states. The energies of hydrogen atoms in a magnetic field are known to a very high precision [9]. The ground state energy of H is maximal in the absence of a magnetic field (-0.5 hartree) and decreases with the growth of the field. At $\gamma=0.2$ a.u. it equals -0.5904 hartree and at $\gamma=0.3$ a.u. it becomes -0.6292 hartree. Corresponding energies of the molecular state $^3\Sigma_u$ at $R\gg 1$ a.u. are -1.1808 hartree and -1.2584 hartree, respectively.

On the other hand, the potential minimum of the singlet state $^1\Sigma_g$ is minimal at $\gamma=0$ and equals -1.1744 hartree. With the growth of the magnetic field the potential minimum also grows [34,35]. The minimum of the triplet state $^3\Sigma_u$, on the contrary, decreases, and already at $\gamma=0.2$ a.u. the energy of the state $^3\Sigma_u$ at $R\gg 1$ a.u. is -1.1808 hartree, i.e., by 0.0064 hartree *lower* than the minimal energy of the state $^1\Sigma_g$ at zero magnetic field and certainly lower than the potential minimum of $^1\Sigma_g$ at $\gamma=0.2$ a.u. As for the state $^3\Pi_u$, in this region of magnetic field strength its potential curve still lies above that of the state $^3\Sigma_u$, which means that $^3\Pi_u$ is an unstable short-lived state.

Therefore, at $\gamma\approx 0.2-0.3$ a.u. the ground state of the hydrogen molecule is not the singlet state $^1\Sigma_g$ or the triplet state $^3\Pi_u$, but the triplet state $^3\Sigma_u$, which is repulsive at $R\sim 1$ a.u. and has a very weak interaction between atoms at large R. This means that with the growth of the magnetic field the hydrogen molecule experiences two transitions of the ground state symmetry. The first transition, which happens at some magnetic field strength $\gamma_1<0.2$ a.u., is the transition from the strongly bound singlet state $^1\Sigma_g$ to the triplet state $^3\Sigma_u$, which is bound very weakly, if at all. The second transition, occurring at a certain $\gamma_2>0.2$ a.u., is the transition from the state $^3\Sigma_u$ to the strongly bound triplet state $^3\Pi_u$.

If the value of γ_2 is large enough, then we are facing the following situation: In *very* strong fields $\gamma>\gamma_2$ the hydrogen forms tightly bound molecules in the state $^3\Pi_u$, but for fields $\gamma\leqslant\gamma_2$ the ground state of the hydrogen is the state $^3\Sigma_u$ with a weak interaction between atoms, which possess large quadrupole moments. Hydrogen behaves like a nonideal Bose gas, and we arrive at the situation described in [28,33].

Recently, a very detailed investigation of singlet and triplet states of the Σ manifold of H_2 in magnetic fields between 0 and 100 a.u. has been published [36]. The authors of [36] performed configuration-interaction (CI) studies of the states $^1\Sigma_g$, $^1\Sigma_u$, $^3\Sigma_g$, and $^3\Sigma_u$. They have found that the ground state of H_2 experiences a symmetry transition from $^1\Sigma_g$ to $^3\Sigma_u$, which happens somewhere between $\gamma=0.1$ and 0.2 a.u., in exact correspondence with the arguments presented above. We have independently reported the same result in Ref. [37], which gives an essential summary of the results which we present in the present paper.

To find the true picture of the ground state evolution, we perform accurate two-dimensional (2D) Hartree-Fock calcu-

lations of the hydrogen molecule in a parallel magnetic field. We solve the problem within the Born-Oppenheimer approximation, which is completely justified for the range of magnetic fields in question, because for hydrogen effects of nonadiabatic corrections become pronounced only in magnetic fields stronger than 10^{11} G for the states with nonzero total momentum [5]. We do not account for relativistic effects due to their negligible influence [10]. Calculations are performed using a highly precise fully numerical method, developed in [38].

Our results demonstrate that the first symmetry transition $^1\Sigma_g \to {}^3\Sigma_u$ occurs at the magnetic field strength of $\gamma_1 \approx 0.18$ a.u., and the second transition $^3\Sigma_u \to {}^3\Pi_u$ happens at $\gamma_2 \approx 14$ a.u. For magnetic fields $\gamma < \gamma_1$ the ground state of the hydrogen molecule is the strongly bound singlet state $^1\Sigma_g$. For magnetic fields $\gamma_1 < \gamma < \gamma_2$ the ground state of H_2 is the triplet state $^3\Sigma_u$ with a very weak interaction between atoms, and the hydrogen must behave like a nonideal Bose gas. For magnetic fields $\gamma > \gamma_2$ the hydrogen forms tightly bound molecules in the quantum state $^3\Pi_u$.

These results provide a solid background to the theory of Bose condensation and superfluidity of a hydrogenlike gas in a strong magnetic field [33] and prove that its assumption of the ground state symmetry is valid. Although the theoretical picture developed in [28,33] does not work for extremely high magnetic fields, as was assumed initially, but for magnetic fields less than 14 a.u., this fact does not change the principal concepts of [33].

In addition, our calculations demonstrate that for $\gamma_1 \leqslant \gamma \leqslant \gamma_2$ there are two regions of magnetic field strength where hydrogen may form *metastable* molecules. The first region lies between γ_1 and ≈ 0.4–0.5 a.u. For magnetic fields of such strength, the true ground state of the molecule is $^3\Sigma_u$, but hydrogen may form strongly bound metastable molecules in the singlet state $^1\Sigma_g$. The second region spans from 1.2–1.4 a.u. to γ_2. In such fields, hydrogen may form metastable molecules in the quantum state $^3\Pi_u$.

This result provides not only qualitative, but also a very good quantitative explanation of experimental results, which were reported in [27] and remained unexplained theoretically. The authors of [27] investigated the excitonic spectrum of germanium in a magnetic field and at $H = 4$ T observed the appearance of a new spectral line, which was labeled the ''*X* line.'' They associated this new line with the creation of a new bound state, whose energy is by one electron-hole (e-h) pair lower than the energy of an isolated exciton, but could not explain the nature of this state.

For the samples of Ge used in the experiments [27] the critical field $H_0^{\rm eff}$ corresponded to 2.9 T. Therefore, the new spectral line appeared at the effective field $\gamma \approx 1.4$ a.u., which approximately corresponds to the lower end of the second metastable region described above. We suggest that the observed *X* line is associated with the metastable exciton in the state $^3\Pi_u$ and predict that other direct-gap semiconductors will exhibit similar spectral features at the same strength of the effective magnetic field. If future experiments with other types of semiconductors confirm this prediction, it will lead to a new way to control the optical properties of semiconductors, which may open interesting technological possibilities.

The paper is organized as follows. In Sec. II, we derive the Hartree-Fock equations and auxiliary formulas in the spheroidal coordinate system. Section III gives the detailed description of the employed numerical method, whose precision and convergence are investigated in Sec. IV. Sections V A and V B present calculated results for the ground state of the magnetized hydrogen molecular ion and for low-lying states of the helium atom. Section V C describes the evolution of the hydrogen molecule in the magnetic field. Section VI presents our explanation of the observed excitonic spectrum of germanium in a strong magnetic field and proposals for future experimental work. Finally, Sec. VII summarizes the contents of the paper and presents our conclusions.

II. HARTREE-FOCK METHOD

A. Basic equations

We use the usual Born-Oppenheimer adiabatic approximation and separate electronic and nuclear motions. The Schrödinger equation for the electronic wave function $\Psi(\mathbf{x}_1,\mathbf{x}_2)$, where $\mathbf{x}_i = (\mathbf{r}_i, s_i)$ collectively designates the space and spin variables of electron i, is

$$[\hat{h}(\mathbf{x}_1) + \hat{h}(\mathbf{x}_2)]\Psi + \frac{e^2}{r_{12}}\Psi = E\Psi, \tag{1}$$

where $r_{12} = |\mathbf{r}_1 - \mathbf{r}_2|$ and $\hat{h}$ is a one-electron Hamiltonian,

$$\hat{h}(\mathbf{x}) = \frac{1}{2m_e}\left[\hat{\mathbf{p}} + \frac{e}{c}\mathbf{A}(\mathbf{r})\right]^2 + \frac{e\hbar}{m_e c}\hat{\mathbf{s}}\mathbf{H} - e^2\sum_{j=1,2}\frac{Z_j}{r_j}. \tag{2}$$

Here $r_j = |\mathbf{r} - \mathbf{R}_j|$ is the distance to the nucleus j, $\mathbf{R}_j$, and Z_j are nuclear coordinates and atomic numbers, $\mathbf{A}$ is the vector potential, $\mathbf{H} = \nabla \times \mathbf{A}$ is the magnetic field, and $\hat{\mathbf{s}}$ is the spin operator. Since the present analysis is restricted to the parallel orientation of the magnetic field, we introduce spheroidal coordinates (ξ, η, φ) with variables $\xi = (r_1 + r_2)/R$, $0 \leqslant \xi < \infty$, and $\eta = (r_1 - r_2)/R$, $-1 \leqslant \eta < 1$, where $R = |\mathbf{R}_1 - \mathbf{R}_2|$ is the internuclear separation. The gauge of the vector potential is taken as $\mathbf{A} = (0, 0, Hr_\perp/2)$, where $r_\perp = (R/2)[(\xi^2 - 1)(1 - \eta^2)]^{1/2}$ is the distance to the molecular axis.

We choose the atomic system of units, so that the units of length and energy are the Bohr radius $a_0 = \hbar^2/m_e e^2 = 5.3 \times 10^{-9}$ cm and 1 hartree, $E_0 = m_e e^4/\hbar^2 = 27.2$ eV, and the unit of magnetic intensity is $H_0 = m_e^2 e^3 c/\hbar^3 = 2.350\,52 \times 10^9$ Oe. The Schrödinger equation (1) takes the form

$$[\hat{h}(\mathbf{r}_1) + \hat{h}(\mathbf{r}_2)]\Psi + \frac{1}{r_{12}}\Psi = (E - \gamma\sigma_1 - \gamma\sigma_2)\Psi, \tag{3}$$

where $\gamma = H/H_0$ is the intensity of the magnetic field in atomic units, $\sigma = s_z = \pm 1/2$ is the z projection of the electron spin, and $\hat{h}$ is the one-electron Hamiltonian without the spin-dependent term,

$$\hat{h}(\mathbf{r}) = -\frac{1}{2}\Delta - i\frac{\gamma}{2}\frac{\partial}{\partial\varphi} + \frac{1}{8}\gamma^2 r_\perp^2 - \frac{2}{R^2}\frac{\mathcal{Z}_p\xi + \mathcal{Z}_m\eta}{\xi^2 - \eta^2}, \tag{4}$$

with $\mathcal{Z}_p = R(Z_1 + Z_2)$ and $\mathcal{Z}_m = R(Z_2 - Z_1)$.

We consider the problem within the Hartree-Fock approximation in which the total electronic wave function

$\Psi(\mathbf{x}_1,\mathbf{x}_2)$ is approximated by the antisymmetrized product of two normalized and orthogonal spin orbitals $\psi_a(\mathbf{r},s)=u_a(\mathbf{r})\chi_a(s)$. The Hartree-Fock equations are

$$[\hat{h}(\mathbf{r})+G_{bb}(\mathbf{r})-E_a]u_a(\mathbf{r})=\delta_s G_{ba}(\mathbf{r})u_b(\mathbf{r}), \tag{5}$$

where indices a and b take values $(a,b)=(1,2)$ and $(2,1)$, E_a are eigenvalues, and $\delta_s=\delta(s_1,s_2)$ is 1 if the electron spins are parallel (triplet term) and 0 if they are antiparallel (singlet term). The potentials G_{ab} are given by

$$G_{ab}(\mathbf{r})=\int \frac{u_a^*(\mathbf{r}')u_b(\mathbf{r}')}{|\mathbf{r}-\mathbf{r}'|}d\mathbf{r}'. \tag{6}$$

B. Transformation to 2D space

We assume that the dependence of the spatial orbitals u_a on the angle φ is given by the factor $e^{im_a\varphi}$, so that the component of the electronic orbital angular momentum along the molecular axis is $\Lambda=m_1+m_2$. We introduce the new functions $f_a(\xi,\eta)$ according to

$$\begin{aligned}u_a(\xi,\eta,\varphi)&=e^{im_a\varphi}r_\perp^{|m_a|}e^{-\alpha\gamma r_\perp^2/4}f_a(\xi,\eta)\\&=e^{im_a\varphi}\phi_a(\xi,\eta),\end{aligned} \tag{7}$$

$$\phi_a(\xi,\eta)=r_\perp^{|m_a|}e^{-\alpha\gamma r_\perp^2/4}f_a(\xi,\eta). \tag{8}$$

The multiplier $\exp(-\alpha\gamma r_\perp^2/4)$, where α ranges between 0 and 1, is introduced to partially account for the asymptotic behavior of the wave function in the magnetic field and is discussed in Sec. III D. The Laplacian of a spatial orbital in spheroidal coordinates is

$$\begin{aligned}\Delta u_a=&\frac{4e^{im_a\varphi}}{R^2(\xi^2-\eta^2)}r_\perp^{|m_a|}e^{-\alpha\gamma r_\perp^2/4}\hat{D}^{(\alpha\gamma)}_{|m_a|}f_a\\&-(1+|m_a|)\alpha\gamma u_a+\alpha^2\gamma^2r_\perp^2u_a/4,\end{aligned} \tag{9}$$

where the differential operator $\hat{D}_n^{(\tau)}$ is defined as

$$\begin{aligned}\hat{D}_n^{(\tau)}(\xi,\eta)=&(\xi^2-1)\frac{\partial^2}{\partial\xi^2}+(1-\eta^2)\frac{\partial^2}{\partial\eta^2}\\&+[2(1+n)-\tau r_\perp^2]\left(\xi\frac{\partial}{\partial\xi}-\eta\frac{\partial}{\partial\eta}\right).\end{aligned} \tag{10}$$

As follows from Eq. (6), the φ dependence of the potentials G_{ab} is given by the factor $e^{i(m_b-m_a)\varphi}$. Consequently, we can present G_{ab} in the form

$$G_{ab}(\xi,\eta,\varphi)=e^{i(m_b-m_a)\varphi}r_\perp^{|m_b-m_a|}g_{ab}(\xi,\eta). \tag{11}$$

The Hartree-Fock equation (5) becomes

$$\begin{aligned}&\hat{D}^{(\alpha\gamma)}_{|m_a|}f_a+(\mathcal{Z}_+\xi+\mathcal{Z}_-\eta)f_a\\&\quad-\frac{R^2}{2}(\xi^2-\eta^2)\left(g_{bb}+\frac{1-\alpha^2}{8}\gamma^2r_\perp^2-E_a'\right)f_a\\&\quad=-\delta_s\frac{R^2}{2}r_\perp^{|m_a-m_b|+|m_b|-|m_a|}(\xi^2-\eta^2)g_{ba}f_b,\end{aligned} \tag{12}$$

where $E_a'=E_a-(\alpha+|m_a|\alpha+m_a)\gamma/2$. Explicit formulas for overlap integrals $S_{ab}=\langle u_a|u_b\rangle$ and Hamiltonian integrals $H_{ab}=\langle u_a|\hat{h}|u_b\rangle$ are given in Appendix A.

To determine the potentials G_{ab}, we follow the method outlined in [38] and directly solve the Poisson equation $\Delta G_{ab}=-4\pi u_a^*u_b$. Written in terms of the functions g_{ab}, it reads

$$\hat{D}^{(0)}_{|m_b-m_a|}g_{ab}=-\pi R^2r_\perp^{-|m_b-m_a|}(\xi^2-\eta^2)\phi_a\phi_b. \tag{13}$$

The values of g_{ab} at the positions of nuclei can be found by direct numerical integration and are given by Eq. (A4). At large distances $\mathbf{R}$ the potentials $G_{ab}(\mathbf{R})$ can be expanded in a multipole series $G_{ab}(\mathbf{R})=\sum_{l=0}^\infty G_{ab}^{(l)}(\mathbf{R})$, where

$$G^{(l)}(\mathbf{R})=\frac{1}{R^{l+1}}\sum_{m=-l}^{l}\sqrt{\frac{4\pi}{2l+1}}Q_m^{(l)}Y_{lm}^*(\Theta,\Phi). \tag{14}$$

Here R, Θ, and Φ are the polar coordinates of $\mathbf{R}$, Y_{lm} are spherical harmonics, and $Q_m^{(l)}$ are multipole moments given by

$$Q_m^{(l)}=\sqrt{\frac{4\pi}{2l+1}}\langle u_a|r^lY_{lm}(\theta,\varphi)|u_b\rangle. \tag{15}$$

Equations (A4) and (A5) give the above multipole expansion in terms of g_{ab}.

Finally, we integrate the Schrödinger equation (3) and obtain the orbital energy E in terms of molecular integrals,

$$\begin{aligned}E=&\gamma\sigma_1+\gamma\sigma_2+H_{11}+H_{22}\\&+\frac{1}{2}[T_{1122}+T_{2211}-\delta_s(T_{1221}+T_{2112})],\end{aligned} \tag{16}$$

where $T_{abcd}=\langle u_a|G_{cd}|u_b\rangle$. The level $E=0$ corresponds to the configuration where all particles are infinitely separated from each other and reside on their lowest Landau levels with spins antiparallel to the magnetic field. The total energy of the molecule is $E_{\rm tot}=E+Z_1Z_2/R$.

III. NUMERICAL SCHEME

A. Coordinate system

To solve the Hartree-Fock equation (12), we approximate functions $f_a(\xi,\eta)$ by their node values on a mesh in the domain $1\leqslant\xi\leqslant\xi_{\max}$, $-1\leqslant\eta\leqslant1$. We do not know the exact form of the boundary conditions on f_a at $\xi\to\infty$ and impose a simplified condition $f_a(\xi_{\max})=0$. Numerical calculations for the field-free molecule ($\gamma=0$) show that this simplification does not appreciably affect results provided that $\xi_{\max}$ is large

enough (see Sec. III C). Coulomb and exchange integrals g_{ab} are also approximated on the same mesh.

The spheroidal coordinate system is not very convenient for numerical integration of Eqs. (12) and (13). First, we should impose boundary conditions at ''practical infinity,'' that is, at $\xi \gg 1$, and the requirement to have a good spatial resolution near the nuclei leads either to a very large number of equally spaced grid points or to a nonuniform grid. Second, if the magnetic field is strong enough, the electron density is sharply concentrated near the molecular axis, and an insufficient density of grid points in this region causes the numerical instability uncovered in our preliminary calculations. Although this instability may be avoided by using a nonuniform grid, such a measure would involve more complicated formulas for numerical differentiation and integration.

Fortunately, both difficulties can be avoided by a suitable transformation of the coordinate system. Instead of working with nonuniform grids in ξ and η, we use equidistant grids in new independent variables t and s, defined in the domains $0 \leqslant t \leqslant T \equiv \ln \xi_{\max}$ and $-1 \leqslant s \leqslant 1$. The connection between $\{\xi, \eta\}$ and $\{t,s\}$ is given by

$$\xi = \exp[T - T\Omega_{\mu_t}(1 - t/T)], \quad \eta = \Omega_{\mu_s}(s), \tag{17}$$

where μ_t and μ_s are adjustable parameters and $\Omega_\mu(x)$ is an odd monotone function defined on $[-1,1]$ and satisfying the conditions $\Omega_\mu(0)=0$, $\Omega_\mu(1)=1$. This function must be chosen so that it will concentrate grid points near $\xi=1$ and $|\eta|=1$. The choice used in this work is $\Omega_\mu(x) = w_\mu(x)/w_\mu(1)$, where

$$w_\mu(x) = \int_0^x (1+\mu^2 z^2)^{-3} dz = \frac{x(5+3\mu^2x^2)}{8(1+\mu^2x^2)^2} + \frac{3}{8\mu}\arctan \mu x. \tag{18}$$

The parameter μ controls the concentration of points: $\mu \approx 0$ results in an almost equidistant grid, and $\mu \sim 2-3$ gives a strongly nonuniform grid.

The differential operator $\hat{D}_n^{(\tau)}$ changes according to usual rules,

$$\hat{D}_n^{(\tau)}(t,s) = (\xi^2-1)t_\xi^2 \frac{\partial^2}{\partial t^2} + (1-\eta^2)s_\eta^2 \frac{\partial^2}{\partial s^2} + [(\xi^2-1)t_{\xi\xi} + (2+2n-\tau r_\perp^2)\xi t_\xi]\frac{\partial}{\partial t} + [(1-\eta^2)s_{\eta\eta} - (2+2n-\tau r_\perp^2)\eta s_\eta]\frac{\partial}{\partial s}, \tag{19}$$

where the subscripts denote derivatives over ξ and η. Double integrals transform as

$$\int_1^{\xi_{\max}} d\xi \int_{-1}^{1} d\eta F(\xi,\eta) = \int_0^T dt \int_{-1}^{1} ds F[\xi(t),\eta(s)]\xi_t \eta_s . \tag{20}$$

The derivatives in Eq. (19) can be expressed as $t_{\xi\xi} = -t_\xi^3 \xi_{tt}$, $t_\xi = 1/\xi_t$, the same for s and η.

We introduce a rectangular grid defined by equidistant points $\{t_i\} = h_t i$ and $\{s_j\} = h_s j - 1$, where indices i and j run from 0 to N_t and N_s, respectively, and the mesh widths are $h_t = T/N_t$ and $h_s = 2/N_s$. Since all numerical integrations are carried out using a five-point approximate formula, the number of intervals in each variable must be a multiple of 4, that is, $N_t = 4n_t$ and $N_s = 4n_s$, where n_t and n_s are integers.

B. Finite-difference formulas

We expressed first and second derivatives of functions u_a and g_{ab} over s and t using the seven-point approximation formulas given in [38]. If we have an equidistant mesh x_i with a constant mesh width $h = x_i - x_{i-1}$ and consider a function $y(x)$ whose node values are $y_i = y(x_i)$, then the first and second derivatives of $y(x)$ at mesh points can be approximated as

$$60hy'(x_i) = \pm \sum_{l=-3}^{3} A_{1+k,4+l} y_{i\pm(k+l)} + \varepsilon_1, \tag{21a}$$

$$180h^2 y''(x_i) = \sum_{l=-3}^{3} B_{1+k,4+l} y_{i\pm(k+l)} + \varepsilon_2, \tag{21b}$$

where $\varepsilon_1 = O(h^8)$ and $\varepsilon_2 = O(h^8)$ for $k=0$ and $O(h^7)$ for $k \neq 0$, and A and B are 4×7 integer matrices given in Appendix B, Eqs. (B1) and (B2). The index $k=0$ gives centered expressions, and $1 \leqslant k \leqslant 3$ generates ''shifted'' formulas, which are used near the mesh boundary. The upper and lower signs in Eqs. (21) correspond to right and left shifts, respectively; an example is given by Eq. (B3).

Numerical integration was done using the five-point Newton-Cotes formula [39] applied to the 5×5 integration grid,

$$\int_{x_i}^{x_{i+4}} y(x)dx = \frac{2h}{45}(7y_i + 32y_{i+1} + 12y_{i+2} + 32y_{i+3} + 7y_{i+4}) + O(h^7). \tag{22}$$

Sometimes, it is convenient to perform initial self-consistent field (SCF) iterations with a small number of grid points and then use the obtained solution as the initial approximation for calculations on a finer grid. To interpolate the functions u_a and g_{ab} to a refined grid with larger N_t and N_s, we used the seven-point Lagrange interpolation formula

$$f(x_i + ph) = \sum_{k=-3}^{3} A_k^7(p) f(x_{i+k}), \tag{23}$$

where $-3 \leqslant p \leqslant 3$ and the interpolation coefficients are [39]

$$A_k^7(p) = (-1)^{k+3} \frac{p(p^2-1)(p^2-4)(p^2-9)}{(3+k)!(3-k)!(p-k)}. \tag{24}$$

C. Self-consistent field iterations

Self-consistent field solutions of the Hartree-Fock equation (12) were obtained by the usual iterative technique. We

start from a certain initial guess of $f_1^{(0)}$ and $f_2^{(0)}$ for the orbitals and $E_1'^{(0)}$ and $E_2'^{(0)}$ for the energy eigenvalues and repeat the following steps of SCF iterations.

(1) Calculate the boundary values of the potentials $g_{ab}^{(k)}$, namely, their values at the positions of nuclei using Eq. (A4) and at practical infinity for $N_t-2\leqslant i\leqslant N_t$ with the aid of multipole expansion (A5) and (A6).

(2) Solve the Poisson equation (13) using any relaxation method. We used the successive overrelaxation (SOR) technique (see, e.g., [40]).

(3) Find new functions $f_a^{(k+1)}$ by solving the Hartree-Fock equation (12) with energy eigenvalues $E_a'^{(k)}$, potentials $g_{ab}^{(k)}$, and orbitals $f_b^{(k)}$. Again, the SOR method is used.

(4) Normalize the spin orbitals $\psi_a^{(k+1)}$. Note that no special orthogonalization is required; if $\delta_s=0$ or $m_a\neq m_b$, the orbitals are automatically orthogonal, and if $\delta_s=1$ and $m_a=m_b$, then one of the orbitals is even and the other one is odd with respect to η.

(5) Calculate new integrals $H^{(k+1)}$ and $T^{(k+1)}$ and new energy eigenvalues $E_a^{(k+1)}=H_{aa}^{(k+1)}+T_{aabb}^{(k+1)}-\delta_s T_{abba}^{(k+1)}$.

(6) If the changes of every orbital $\|f_a^{(k+1)}-f_a^{(k)}\|$ and every energy eigenvalue $\|E_a^{(k+1)}-E_a^{(k)}\|$ are less than certain predefined values, we consider the solution as converged and stop the SCF iterations; otherwise, we return to step (1).

The above scheme requires several comments. First of all, it is necessary to specify the boundary conditions which we impose on the functions $f_a(\xi,\eta)$ when solving the Hartree-Fock equation (12). Since we do not know the exact asymptotic behavior of the functions f_a at infinity, we simply put f_a to zero at $N_t-2\leqslant i\leqslant N_t$. Calculations in the field-free case show that this simplification does not produce any noticeable effect if $\xi_{\max}$ is sufficiently large. A judicious estimate of the required $\xi_{\max}$ can be obtained from the following reasoning.

Taken with the opposite sign, an eigenvalue E_a of the Hartree-Fock equation (5) represents the energy required to remove the ath electron from the molecule on the assumption that f_b for the molecular ion is the same as for the molecule. In the presence of a magnetic field this ''ionization'' energy is $\gamma/2-E_a$. If we now assume that the asymptotic behavior of the orbital f_a along the field is approximately $\exp(r\sqrt{\gamma-2E_a})$ (see [9], Sec. IV) and that it is safe to set f_a to zero where it is less than, say, 10^{-K}, $K\sim 10-12$, then we immediately obtain that a ''sufficiently large'' $\xi_{\max}$ is

$$\xi_{\max}=\max_a \frac{2K\ \ln 10}{R\sqrt{\gamma-2E_a}}. \tag{25}$$

For example, if we take $K=10$ and consider the ground molecular state $^3\Pi_0$ $(\Lambda=-1)$ in the field $\gamma=1$ a.u., then $\xi_{\max}$ given by Eq. (25) corresponds to the spatial distance $r_{\max}=(R/2)\xi_{\max}\approx 17$ a.u.

Along with the boundary conditions at practical infinity we must also set conditions near the nuclei. This is done in the following manner. If $m_a=0$, then during the SOR recalculation of $f_a^{(k+1)}$ we do not change the value of $f_a^{(k+1)}$ at the position of one or both of the nuclei, depending on the required η symmetry of the orbital (if $\delta_s=0$ or $m_a\neq m_b$, then we do not impose the requirement of η symmetry at large R in order to obtain correct results in the dissociation limit). For $m_a\neq 0$ we choose a ''fixed point'' somewhere in the vicinity of a nucleus (usually at $i=j=3,...,5$). Of course, during the normalization of the recalculated functions $f_a^{(k+1)}$ all node values are changed, including those that were kept constant during the SOR calculation.

A marked feature of the employed computational method is the high sensitivity of SCF iterations to the initial choice of eigenvalues $E_a^{(0)}$ and functions $f_a^{(0)}$. If the starting guess is far from the true solution, then SCF iterations immediately diverge. The state $^1\Sigma_0$ $(\Lambda=0)$ is less prone to this instability, but for the state $^3\Pi_0$ $(\Lambda=-1)$ in strong and superstrong magnetic fields it is a severe problem. Luckily, this difficulty may be obviated by systematic construction of the starting functions $f_a^{(0)}$, ''damping'' of several initial iterations, and setting parameter α to a nonzero value (see Sec. III D).

Spatial orbitals u_a must satisfy the cusp condition at the positions of nuclei, have the correct asymptotic behavior along the field lines, and decay as $\exp(-\gamma r_\perp^2/4)$ in the transverse direction. In addition, our approximate boundary condition at infinity requires the orbitals to become zero at $i\geqslant N_t-2$. All these demands may be met if we initialize the functions $f_a^{(0)}$ as

$$f_a^{(0)}=\frac{\xi^*-\xi}{\xi^*-1}\exp\left[-\frac{(1+\lambda_a r)r}{1+|m_a|+r}-\frac{1-\alpha}{4}\gamma r_\perp^2\right], \tag{26}$$

where $\lambda_a=[\gamma(1-\alpha)(1+|m_a|)-2E_a]^{1/2}$, ξ^* is the value of ξ at $i=N_t-2$ ($f_a\equiv 0$ for $i\geqslant N_t-2$), and $r=(R/2)(\xi\pm\eta)$ is the distance from a chosen nucleus. Obtained in such a way, the functions f_a are (if necessary) η symmetrized and normalized.

To improve the stability of SCF iterations on the initial stage, the eigenvalues $E_a^{(1)}$, $E_a^{(2)}$, and $E_a^{(3)}$ are recalculated according to

$$E_a^{(k+1)}=\varepsilon_k[H_{aa}^{(k+1)}+T_{aabb}^{(k+1)}-\delta_s T_{abba}^{(k+1)}]+(1-\varepsilon_k)E_a^{(k)}, \tag{27}$$

where the parameter ε_k controls the ''damping'' of rapid changes which can occur on starting. Usually we used values $\varepsilon_0=0.2$, $\varepsilon_1=0.5$, and $\varepsilon_2=0.8$.

Both SOR and SCF iterations approach exact solutions (here we understand the word ''exact'' in the finite-difference context) exponentially but never actually reach them. Therefore, we must terminate iterations when certain predefined convergence criteria become true. In the case of SOR, the stopping criterion may be easily defined as the average residual per node. However, SCF iterations do not provide such a convenient measure of convergence. Instead, we use changes of the orbitals $\|u_a^{(k+1)}-u_a^{(k)}\|$ and eigenvalues $|E_a^{(k+1)}-E_a^{(k)}|$ and terminate calculations when these quantities fall below preset limits.

D. Stability of the method

The SOR technique used here for the calculation of potentials and wave functions is well documented in the literature. In the case of the usual three-point approximations of first and second derivatives its application usually presents

TABLE I. Difference $E(N_t,N_s)-E_{\text{exact}}$ (in nhartree) for the ground states of the hydrogen atom, hydrogen molecular ion, and the hydrogen molecule as a function of the grid size. The parameters R and $r_{\max}$ are given in the table, $\mu_t=\mu_s=0.1$.

N_t	$N_s=24$	$N_s=32$	$N_s=40$	$N_s=48$
H ($R=2.0$ a.u., $r_{\max}=20$ a.u., $E_{\text{exact}}=-0.5$)				
24	516.2	515.6	515.5	515.5
40	−7.7	−8.4	−8.5	−8.5
56	−1.1	−1.7	−1.8	−1.8
72	0.3	−0.3	−0.4	−0.4
80	0.5	−0.1	−0.2	−0.2
88	0.6	0.0	−0.1	−0.1
96	0.6	0.0	−0.1	−0.1
H_2^+ ($R=2.0$ a.u., $r_{\max}=15$ a.u., $E_{\text{exact}}=-1.102\,634\,214\,5$)				
24	2887.4	2886.4	2886.2	2886.2
40	38.0	36.9	36.8	36.8
56	2.4	1.3	1.2	1.1
72	1.2	0.1	−0.1	−0.1
80	1.1	0.1	−0.1	−0.1
H_2 ($R=1.4$ a.u., $r_{\max}=20$ a.u., $E_{\text{exact}}=-1.133\,629\,57$)				
24	6074.0	6070.4	6069.2	6068.4
40	186.7	185.5	185.9	186.3
56	17.3	15.5	15.4	15.5
72	3.3	1.4	1.3	1.3
88	1.2	−0.7	−0.8	−0.8
104	1.0	−1.2	−1.3	−1.3
112	0.8	−1.3	−1.4	−1.4
120	0.7	−1.3	−1.4	−1.4

no difficulties in terms of numerical stability. It turned out, however, that for the seven-point approximation formulas stability of the successive overrelaxation method strongly depends on the order in which we recalculate node values during SOR iterations.

When we use the usual three-point approximation formulas, then even the simplest algorithm, which recalculates values at nodes (i,j) with i running from 0 to N_t and j running from 0 to N_s for every i, works without faults. However, in our case of seven-point formulas this trivial scheme happened to be unstable. Fortunately, the problem can be cured by a simple modification of the order in which the node values are recalculated: SOR iterations become stable when the index i runs first from 0 to $N_t/2$ and then back from N_t to $N_t/2$, and the index j, in a similar manner, runs first from 0 to $N_s/2$ and then backwards from N_s to $N_s/2$ for each i.

Another potential source of divergence is the quadratic term $\gamma^2 r_\perp^2$ in the one-electron Hamiltonian (4), which tends to create numerical instability if the magnetic intensity γ is large. To overcome this problem, we introduced several procedures for the improvement of the convergence.

The first and the most pronounced instability usually observed at large γ is the instability of SOR iterations which develops in the area $|\eta|\approx 1$. This instability is triggered by an insufficient density of grid points η_j and can be suppressed either by increasing the number N_s of grid points or by increasing the parameter μ_s, since both measures create a concentration of points on the η axis in the troublesome region $|\eta|\approx 1$. However, the first method increases the number of nodes, thus significantly slowing down the speed of computation, while the second one solves the problem by shifting nodes closer to the molecular axis. This measure is usually more efficient because in the presence of a magnetic field the wave function is concentrated along the field lines, and by increasing μ_s we adapt the grid to the new physical situation. Typically, we use $\mu_s=1$ for $\gamma=1$ and $\mu_s=3-4$ for $\gamma=10^{2-3}$.

The second stability problem caused by a large γ is the increased sensitivity of SCF iterations to the initial choice of spatial orbitals $f_a^{(0)}$ and eigenvalues E_a^0, which was already discussed in the preceding section. This problem develops if the parameter α, which defines the partial separation of magnetic asymptote $\exp(-\alpha\gamma r_\perp^2/4)$ in Eq. (7), is zero or close to zero. However, SCF iterations are completely stabilized by increasing α to 0.1–0.3, although this measure results in a larger number of iteration steps. We did not observe any appreciable effect of the value of α on the accuracy of the final converged results.

A side effect resulting from the introduction of a nonzero α is the instability of SOR iterations at large $r_\perp$. To get rid of this problem, the functions $f_a^{(k+1)}$ are recalculated according to the modified Hartree-Fock equations

$$\begin{aligned}\hat{D}^{(\sigma\alpha\gamma)}_{|m_a|} f_a^{(k+1)} &+ (\mathcal{Z}_+\xi+\mathcal{Z}_-\eta) f_a^{(k+1)} \\ &- \frac{R^2}{2}(\xi^2-\eta^2)\left(g_{bb}+\frac{1-\alpha^2}{8}\gamma^2 r_\perp^2 - E_a'\right) f_a^{(k+1)} \\ &= -\delta_s \frac{R^2}{2} r_\perp^{|m_a-m_b|+|m_b|-|m_a|}(\xi^2-\eta^2) g_{ba} f_b^{(k)} \\ &+ (1-\sigma)\alpha\gamma r_\perp^2\left(\xi\frac{\partial}{\partial\xi}f_a^{(k)} - \eta\frac{\partial}{\partial\eta}f_a^{(k)}\right), \end{aligned} \tag{28}$$

where the potentials and eigenvalues are calculated from the kth step of SCF iterations. Stabilization of the α-induced SOR divergence is achieved by the introduction of the parameter σ whose typical value lies between 0.5 and 1; usually, we used $\sigma=1-\alpha$.

IV. CONVERGENCE AND TESTS

In order to check the reliability and convergence properties of the present technique, we performed calculations for several simplest one- and two-electron systems which were already investigated previously by independent methods. We start with the field-free situation, where we consider two one-electron problems, the hydrogen atom H and the hydrogen molecular ion H_2^+, and two two-electron problems, the hydrogen molecule H_2 and the helium atom He. Table I shows the difference between the energy values $E(N_t,N_s)$ obtained by the current method and the best available benchmarks E_{exact} for the ground states of H, H_2^+, and H_2. The energy difference is given in nhartree (1 nhartree = 10^{-9} hartree) as a function of N_t and N_s. The internuclear distance R is 2.0 a.u. for H and H_2^+ (of course, for the atom the term ''internuclear'' refers only to the coordinate system) and 1.4 a.u. for the hydrogen molecule in singlet state. In each case the outer radius $r_{\max}=(R/2)\xi_{\max}$ was determined according to Eq. (25) with $N\approx 8$ and is given in Table I. Exact ground

TABLE II. Convergence of results $E(N_t,N_s)-E_{\text{exact}}$ for the ground state of the helium atom in the absence of a magnetic field. The ''internuclear'' distance is $R=1.4$ a.u., $r_{\max}=15$ a.u., $\mu_t=\mu_s=0.1$. The difference is given in nhartree.

N_t	$N_s=32$	$N_s=56$	$N_s=72$	$N_s=88$	$N_s=104$
24	−4985.1	−5383.4	−5467.0	−5523.6	−5565.9
40	319.6	145.4	139.6	137.4	136.1
56	202.7	36.1	32.3	31.6	31.4
72	177.2	12.0	8.5	7.9	7.8
88	171.0	6.6	3.1	2.5	2.4
104	169.0	5.1	1.6	1.0	0.9
112	168.4	4.8	1.3	0.7	0.6
120	168.1	4.6	1.1	0.5	0.4

state energy values are -0.5 hartree for H, $-1.102\,634\,214\,494\,9$ hartree for H_2^+ (Ref. [41]), and $-1.133\,629\,57$ hartree for H_2 (Ref. [38]).

As we see, convergence of the method is excellent. In all three cases results steadily converge both in N_t and N_s and, for the one-electron systems, fall within 10^{-10} hartree of the exact solution. For the hydrogen molecule, the precision of our results seems to slightly exceed that of Ref. [38], and we can put the Hartree-Fock limit for this system to $-1.133\,629\,571(1)$ hartree. Notice that, unlike variational calculations, the fully numerical method gives energies that are not necessarily upper bounds on the exact values.

Convergence of the ground state of the helium atom is shown in Table II (the exact value given in Ref. [42] is $-2.861\,679\,995\,612\,2$). Again, the fully numerical method gives an accuracy better than 10^{-9} hartree, although this time the convergence in N_s is considerably slower than for H_2.

Convergence of the method in the presence of magnetic field is illustrated by the examples of the hydrogen atom H and the hydrogen molecule H_2. Table III lists the differences between the calculated ground state energies of the hydrogen atom in a magnetic field and the corresponding exact values taken from Ref. [9]. For $\gamma=1.0$ a.u. ($E_{\text{exact}}=-0.831\,168\,896\,733$ hartree) convergence is excellent, and $N_t=N_s=120$ gives fully numerical results accurate to within 10^{-10} hartree. If the field is increased to $\gamma=100.0$ a.u., convergence of the present method becomes slower: The energy calculated at $N_t=80$ and $N_s=120$ differs from the exact value $-3.789\,804\,236\,305$ hartree by more than 10^{-7} hartree.

TABLE III. Difference $E(N_t,N_s)-E_{\text{exact}}$ for the ground state of the hydrogen atom in magnetic field. Results for $\gamma=1$ a.u. are calculated at $R=2.0$ a.u., $r_{\max}=15$ a.u., $\mu_s=1.0$, and $\alpha=0.3$; calculations for $\gamma=100$ a.u. were performed at $R=0.7$ a.u., $r_{\max}=7$ a.u., $\mu_s=3.0$, and $\alpha=0.1$. In both cases $\mu_t=0.1$.

N_t	$N_s=40$	$N_s=56$	$N_s=80$	$N_s=104$	$N_s=120$
			$\gamma=1$ a.u., ΔE in nhartree		
24	−788.88	−874.80	−884.55	−885.33	−885.42
40	67.36	−18.55	−28.31	−29.08	−29.18
64	95.46	9.54	−0.21	−0.99	−1.09
88	96.51	10.59	0.84	0.06	−0.03
104	96.60	10.68	0.93	0.16	0.06
120	96.63	10.71	0.96	0.18	0.09
			$\gamma=100$ a.u., ΔE in μhartree		
24	−29 204.6	−29 104.5	−29 088.8	−29 087.1	−29 086.8
40	−959.6	−859.2	−843.4	−841.7	−841.4
56	−158.0	−57.5	−41.7	−40.0	−39.7
72	−120.3	−19.8	−4.0	−2.3	−2.0
80	−118.5	−18.0	−2.2	−0.5	−0.2

TABLE IV. Convergence of the calculated energy eignevalues $E(N,N)$ for two different quantum states of H_2 in a magnetic field: $^1\Sigma_g$ in a field $\gamma=1.0$ a.u. ($R=1.22$ a.u.) and $^3\Pi_u$ ($\Lambda=-1$) in a field $\gamma=20.0$ a.u. ($R=0.64$ a.u.). Values of R are close to the corresponding equilibrium distances, the parameters $r_{\max}$ and μ_s are given in the table, and $\alpha=1-\sigma=0.3$ and $\mu_t=0.1$ in both cases. Calculations for $^1\Sigma_g$ are done for two different values of $r_{\max}$, 15 and 20 a.u.

N	E	N	E
	$^1\Sigma_g$, $\gamma=1.0$ ($r_{\max}=15$ a.u., $\mu_s=1.0$)		
24	−0.847 590 294 7	80	−0.847 594 785 6
32	−0.847 593 709 7	88	−0.847 594 786 5
40	−0.847 594 539 0	96	−0.847 594 787 0
48	−0.847 594 717 3	104	−0.847 594 787 2
56	−0.847 594 763 7	112	−0.847 594 787 3
64	−0.847 594 778 3	120	−0.847 594 787 4
72	−0.847 594 783 5		
	The same, $r_{\max}=20$ a.u.		
24	−1.847 586 952 6	80	−1.847 594 784 7
32	−1.847 593 144 9	88	−1.847 594 786 1
40	−1.847 594 407 8	96	−1.847 594 786 7
48	−1.847 594 680 0	104	−1.847 594 787 1
56	−1.847 594 751 3	112	−1.847 594 787 3
64	−1.847 594 773 5	120	−1.847 594 787 4
72	−1.847 594 781 5		
	$^3\Pi_u$ ($\Lambda=-1$), $\gamma=20.0$ ($r_{\max}=10$ a.u., $\mu_s=1.5$)		
24	−4.495 906 352	80	−4.495 298 026
48	−4.495 291 246	88	−4.495 299 075
56	−4.495 293 164	96	−4.495 299 938
64	−4.495 295 122	104	−4.495 300 658
72	−4.495 296 732		

Table IV lists energy eigenvalues for the hydrogen molecule which were computed at several $N_t=N_s=N$. The eigenvalues were calculated for two different symmetry states of the molecule, $^1\Sigma_g$ and $^3\Pi_u$, at two different field strengths, $\gamma=1$ a.u. and $\gamma=20$ a.u., respectively. The internuclear distances R are close to the equilibrium values. As in the case of a single hydrogen atom, convergence of eigenvalues at $\gamma=1$ a.u. is excellent, while at $\gamma=20$ a.u. the difference between the last two values is still larger than 10^{-7} hartree.

It is useful to perform a more detailed analysis of convergence. Let us return to the field-free helium atom (Table II) and investigate eigenvalues calculated with $N_t=112$ and different N_s. Open circles in Fig. 1 show the difference $E(112,N_s-8)-E(112,N_s)$ plotted as a function of the index N_s. The logarithmic scale of both axes reveals that the difference accurately obeys a power law dependence. The same

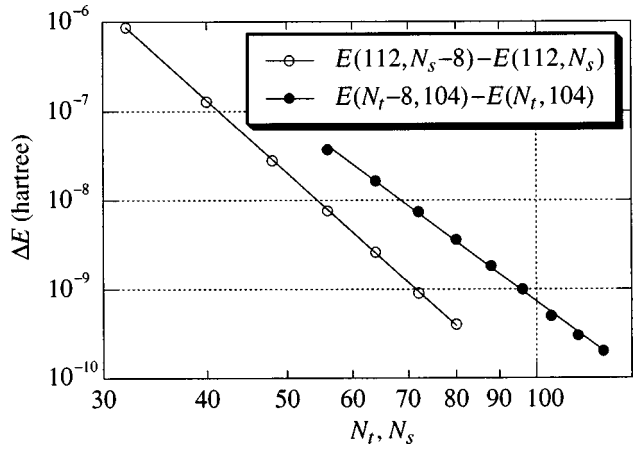

FIG. 1. Convergence of the energy eigenvalue for the ground state of the helium atom in the absence of a magnetic field. Open circles show the difference (in hartree) between pairs of eigenvalues calculated with the same $N_t=112$ and different N_s as a function of N_s. Solid circles show the difference between pairs $E(N_t,N_s=108)$ and $E(N_t-8,N_s=108)$ versus N_t. Solid lines represent fittings of results using the power law.

result is observed for eigenvalues calculated with $N_s=104$ and different N_t: The difference $E(N_t-8,104)-E(N_t,104)$ plotted in Fig. 1 as solid circles also fits a straight line.

Fitting of the results shown in Fig. 1 gives the following approximate formulas:

$$E(112,N_s)-E(112,N_s-8)\approx -3.7\times 10^6 N_s^{-8.4},$$

$$E(N_t,104)-E(N_t-8,104)\approx -7\times 10^4 N_t^{-7}.$$

Although errors in the eigenvalues are not directly related to the truncation errors of finite-difference formulas, which behave like $O(h^7)$ or $O(h^8)$, they follow the power law tendency very accurately. As a result, we can reliably extrapolate the eigenvalues to infinite N_t and N_s. If we consider a series E_n, which obeys the relationship $E_n-E_{n-k}=an^{-b}$, $b>1$, and use the trivial inequality

$$\int_{n-k}^{n}(x+k)^{-b}dx<kn^{-b}<\int_{n-k}^{n}x^{-b}dx, \tag{29}$$

then summation over n yields upper and lower bounds on the error,

$$\frac{a}{(n+k)^{b-1}}<k(b-1)(E_\infty-E_n)<\frac{a}{n^{b-1}}. \tag{30}$$

The coefficients a and b can be easily computed if we know three subsequent terms E_{n-2k}, E_{n-k}, and E_n,

$$b=\log_{n/(n-k)}\frac{E_{n-k}-E_{n-2k}}{E_n-E_{n-k}},$$

$$a=(E_n-E_{n-k})n^b, \tag{31}$$

and we obtain a convenient formula

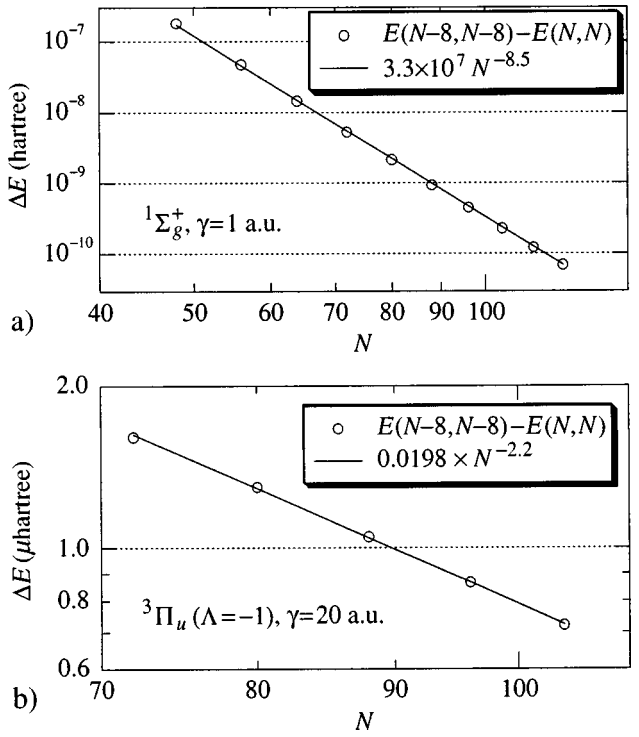

FIG. 2. Convergence of the energy eigenvalues for H_2 in a magnetic field γ. (a) $^1\Sigma_g$, $\gamma=1$ a.u., $r_{\max}=15$ a.u. (b) $^3\Pi_u$, $\gamma=20$ a.u.

$$E_\infty=E_n+\frac{n}{k(b-1)}(E_n-E_{n-k})\,\delta, \tag{32}$$

where

$$\left(\frac{n}{n+k}\right)^{b-1}<\delta<1. \tag{33}$$

Let us now check if the uncovered dependence holds in the presence of a magnetic field. We shall use eigenvalues for the hydrogen molecule presented in Table IV. Figure 2 shows that even in this case differences between successive eigenvalues decrease according to a power law dependence. However, the exponents are different. For $\gamma=1$ a.u., the dependence is described by

$$E(N-8,N-8)-E(N,N)\approx 3.3\times 10^7 N^{-8.5}, \tag{34}$$

and for $\gamma=20$ a.u. the corresponding formula is

$$E(N-8,N-8)-E(N,N)\approx 0.02N^{-2.2}. \tag{35}$$

The decrease of the convergence rate with the growth of γ is explained by the fact that the mesh used at $\gamma=20$ a.u. is significantly more inhomogeneous ($\mu_s=1.5$) than at $\gamma=1$ a.u. ($\mu_s=1.0$). Consequently, the mesh width depends on N nonlinearly, which is seen in the behavior of eigenvalues giving an integrated measure of the approximation errors. The important fact, however, is that Eqs. (32) and (33) are still valid.

Finally, we must investigate the convergence of results with the growth of $r_{\max}$. If we will increase $r_{\max}$ and simultaneously keep N constant, the mesh width will grow and the approximation errors will increase. Therefore, we must cal-

TABLE V. Accurate ground state eigenvalues for the hydrogen molecular ion in a magnetic field γ. The internuclear distance R is selected to be close to the equilibrium configuration. Results are valid to ± 1 in the last quoted digit.

γ	R (a.u.)	$E(R)$(hartree)
1	1.7	−1.562 967 873
10	1.0	−3.173 722 18
100	0.5	−7.127 630 5
1000	0.2	−16.359 853

culate $E_\infty(r_{\max})=\lim_{N\to\infty}E(N,r_{\max})$ for different $r_{\max}$. We have performed such calculations for the singlet state $^1\Sigma_g$ in the magnetic field $\gamma=1.0$ a.u. with two different values of $r_{\max}$, 15 and 20 a.u. The results are listed in Table IV. The first value $r_{\max}=15$ a.u. corresponds to the decay exponent $K=8.93$ [see Eq. (25)], the second value $r_{\max}=20$ a.u. to $K=11.9$ ($\gamma-2E_1=1.88$ hartree). As the mesh size N grows, both eigenvalues converge to within 10^{-10} hartree.

V. RESULTS

A. Hydrogen molecular ion H_2^+

The energy levels of the hydrogen molecular ion H_2^+ in an external magnetic field were extensively investigated for a wide region of magnetic field strength [24,43,25], from superstrong [44,45,21] and intermediate fields [22,26] to the low-field regime [23]. However, the accuracy of the results obtained for $\gamma\geqslant 1$ a.u. usually did not exceed 10^{-5}–10^{-6} hartree. Since highly accurate benchmark results are clearly of interest for testing new computational methods and computer codes, we used the present method to obtain a series of precise results for the ground state of H_2^+ at different strengths of the applied magnetic field. These results, which are listed in Table V, were already used to investigate the accuracy and convergence of modified Gaussian basis sets for calculations in strong magnetic fields [46]. The internuclear distances are chosen to be close to the equilibrium distances reported in [21,25].

B. Helium atom in a magnetic field

If we set Z_1 to 2 and Z_2 to zero, we can compute Hartree-Fock energy levels for the helium atom in a magnetic field. Such calculations may serve as an additional check of our computational technique, because we can compare our results with the accurate Hartree-Fock values reported in [15]. Since the helium atom is not the core of the present analysis, we have restricted the calculations to the states $1\,^1S_0$ (the ground state in the absence of magnetic field) and $2\,^3P_{-1}$ (the ground state of He in strong magnetic fields $\gamma\gg 1$) and to several values of γ. Our results, together with the values from [15], are presented in Table VI. As we see, agreement with previous results is excellent, and the discrepancy is typically less than 1 mhartree.

C. Hydrogen molecule H_2

Let us now turn to the problem of the hydrogen molecule in a parallel magnetic field. We start from the region of low magnetic fields and follow the evolution of the potential curves $^1\Sigma_g$, $^3\Sigma_u$, and $^3\Pi_u$ as the magnetic field grows. For the triplet states, we consider only the lowest triplet component, that is, the one with total electronic spin $S_z=-1$.

TABLE VI. Hartree-Fock binding energies (in a.u.) of the states $1\,^1S_0$ and $2\,^3P_{-1}$ of the helium atom in a magnetic field γ (a.u.). For a comparison, we present the corresponding energy values from Ref. [15].

γ	$1\,^1S_0$	$2\,^3P_{-1}$
0.1	2.959 709 36	2.258 4
	2.960 0[a]	2.259 3[a]
0.2	3.053 844 87	2.361 7
	3.054 1[a]	2.361 9[a]
0.5	3.314 450 94	2.615 49
	3.314 8[a]	2.616 2[a]
1	3.688 884 85	2.959 665
	3.689 1[a]	2.959 9[a]
2	4.289 144 42	3.502 028
	4.289 1[a]	3.502 2[a]
5	5.532 445 1	4.617 21
	5.532 6[a]	4.617 3[a]
10	6.889 366 2	5.829 49
	6.889 6[a]	5.829 5[a]
20	8.680 391 2	7.427 66
	8.680 6[a]	7.427 7[a]
50	11.856 093	10.264 46
	11.856 5[a]	10.264 4[a]
100	14.995 822	
	14.997 4[a]	
200	18.893 61	
	18.894 6[a]	

[a]Values from Ref. [15].

Figure 3 shows the behavior of the potential curves $^1\Sigma_g$, $^3\Sigma_u$, and $^3\Pi_u$ of H_2 as the magnetic field grows from 0 to 0.5 a.u. This region of magnetic field strength encompasses several important effects. First of all, at $\gamma\approx 0.2$ a.u. the hydrogen molecule undergoes the first transition of its ground state symmetry from the strongly bound singlet state $^1\Sigma_g$ to the triplet state $^3\Sigma_u$, characterized by an extremely weak interaction between atoms in the molecule. However, this transition does not imply that the singlet state $^1\Sigma_g$ immediately disappears from the picture. Instead, as the magnetic field continues to grow from $\gamma\approx 0.2$ a.u. to $\gamma\approx 0.4$ a.u., the state $^1\Sigma_g$ remains a metastable state of the system. Finally, as the magnetic field reaches $\gamma\approx 0.4$ a.u., the singlet state $^1\Sigma_g$ becomes a short-lived unstable state of the molecule. At $\gamma=0.5$ a.u., the hydrogen molecule does not have any stable or metastable states which are strongly bound, which means that the molecule must consist of two separated and weakly interacting atoms.

Figure 3(a) presents the classical picture of the potential curves of the hydrogen molecule in the absence of a magnetic field. Solid curves show the energy in the Hartree-Fock approximation, and dashed curves correspond to the total energy with account taken of the electron correlation, from [47]. The correlation energy is significant for the singlet state $^1\Sigma_g$ but is much smaller for the triplet states, which is ex-

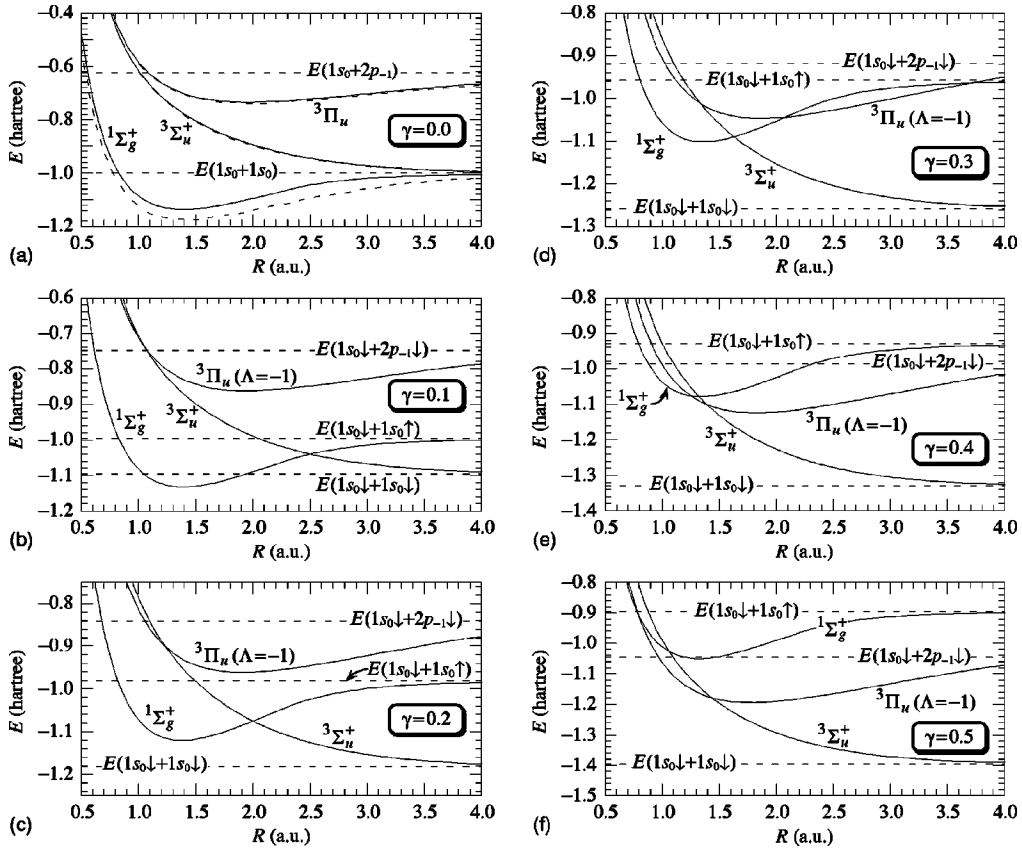

FIG. 3. Potential curves of the quantum states $^1\Sigma_g$, $^3\Sigma_u$, and $^3\Pi_u$ in a parallel magnetic field between 0.0 and 0.5 a.u. Solid curves show Hartree-Fock results; dotted curves are exact solutions. Dotted lines show energies of states in the limit $R\to\infty$.

plained by the smaller overlap of electronic orbitals in triplet states.

To investigate the behavior of the correlation energy with the growth of the magnetic field strength, we can compare our numbers with the results of the elaborate CI calculations performed in [36]. At $\gamma=0.5$ and equilibrium internuclear distance $R=1.33$ a.u., our Hartree-Fock energy for $^1\Sigma_g$ is -1.0479 hartree, CI energy from [36] is -1.0891 hartree, and the correlation energy is 0.0412 hartree; at $\gamma=1.0$ a.u. and $R=1.24$ a.u., the Hartree-Fock energy is -0.8474 hartree and CI energy is -0.8903 hartree, which gives a correlation energy of 0.0429 hartree. If we compare these results with the field-free correlation energy of H_2, equal to 0.0408 hartree at $R=1.4$ a.u., we see that, at least for magnetic fields up to 1 a.u., the correlation energy of the hydrogen molecule in the singlet state $^1\Sigma_g$ remains approximately the same. Analysis of the correlation energy of the triplet state $^3\Sigma_u$ gives similar results.

Figure 3(b) shows the potential curves of the same states $^1\Sigma_g$, $^3\Sigma_u$, and $^3\Pi_u$ in a magnetic field $\gamma=0.1$ a.u. (for $\gamma\neq0$ we show only the Hartree-Fock energies). The potential well of the state $^3\Pi_u$ has become slightly deeper, but it lies high above the curve of the triplet state $^3\Sigma_u$. The curve of $^3\Sigma_u$ has been shifted lower due to the increase in the binding energy of separated hydrogen atoms. The singlet state $^1\Sigma_g$ has stayed almost at the same place, because the decrease in its potential energy due to the deformation of the wave function is compensated for by the interaction of the electron spins with the magnetic field. As a result, the HF energy of $^1\Sigma_g$ in its minimum position $R\approx1.4$ a.u. is -1.1298 hartree, i.e., by 0.0038 hartree higher than the field-free value of -1.1336 hartree. The energy of the triplet state $^3\Sigma_u$ at $R\gg1$ is -1.0951 hartree, and the state $^1\Sigma_g$ is still the ground state.

When the field increases to $\gamma=0.2$ a.u., the situation changes dramatically. Figure 3(c) demonstrates that the minimum of the HF energy of the singlet state $^1\Sigma_g$ becomes higher than the energy of the triplet state $^3\Sigma_u$ at $R\gg1$, while the second triplet state $^3\Pi_u$ is still sufficiently high. It means that now the ground state of the system is the triplet state $^3\Sigma_u$ with a very weak interaction between atoms, and hydrogen behaves like a gas of weakly interacting atoms. The results of [36] show that this result holds when we include the electron correlation.

Although the singlet state $^1\Sigma_g$ has lost its position as the ground state, one can immediately see the possibility for the formation of *metastable* molecules in the state $^1\Sigma_g$. The potential minimum of $^1\Sigma_g$ at $\gamma=0.2$ a.u. is located at $R\approx1.38$ a.u., while the crossing of the HF curves $^1\Sigma_g$ and $^3\Sigma_u$ occurs at $R\approx2.0$ a.u. (with account for the electron correlation, the latter distance becomes even larger). Therefore, a molecule formed in the potential minimum of $^1\Sigma_g$ remains in this state until it is destroyed by some external mechanism, like a collision with another molecule.

In a magnetic field $\gamma=0.3$ a.u. the picture of the potential curves remains essentially the same as at $\gamma=0.2$. This is shown in Fig. 3(d). The ground state of the system is the triplet state $^3\Sigma_u$, the singlet state $^1\Sigma_g$ is a metastable state, and the triplet state $^3\Pi_u$ is an unstable short-lived state.

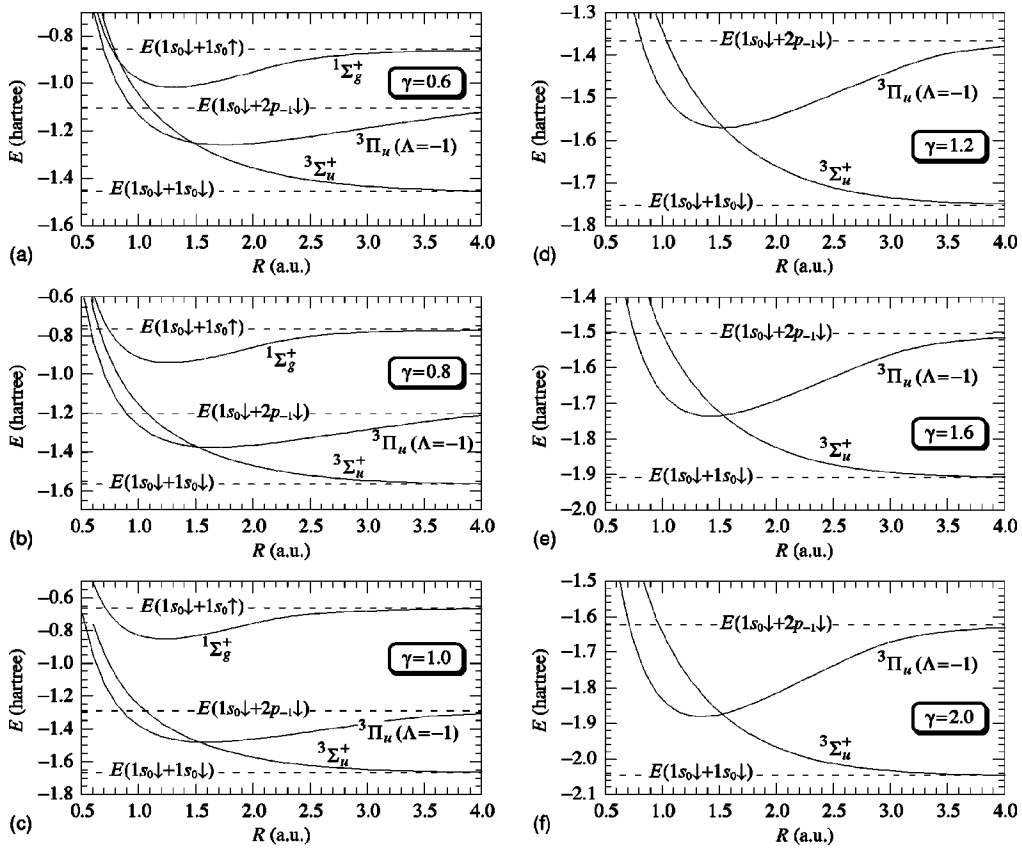

FIG. 4. Hartree-Fock potential curves of the quantum states $^1\Sigma_g$, $^3\Sigma_u$, and $^3\Pi_u$ in a magnetic field between 0.6 and 2.0 a.u.

However, at $\gamma=0.4$ a.u. the situation changes. Figure 3(e) demonstrates that at this field strength the position of the potential minimum of the singlet state $^1\Sigma_g$ almost coincides with the point of intersection of the curves $^1\Sigma_g$ and $^3\Sigma_u$. This means that the lifetime of the molecule in the metastable state $^1\Sigma_g$ becomes very short. The state $^1\Sigma_g$ changes from a metastable to a short-lived unstable state.

This change becomes perfectly clear when we look at Fig. 3(f), which shows the behavior of the potential curves in a magnetic field $\gamma=0.5$ a.u. The potential minima of both the singlet state $^1\Sigma_g$ and the triplet state $^3\Pi_u$ lie above the curve of the ground state $^3\Sigma_u$. There is no possibility for the formation of strongly bound metastable molecules, and all hydrogen molecules are in the ground state $^3\Sigma_u$, which means that hydrogen presents a gas of weakly interacting atoms.

Let us proceed to Fig. 4 and follow the evolution of the potential curves of H_2 as the magnetic field grows to 2 a.u. When we look at Figs. 4(a)–4(c), which show the potential curves $^1\Sigma_g$, $^3\Sigma_u$, and $^3\Pi_u$ in magnetic fields $\gamma=0.6$ a.u., 0.8 a.u., and 1.0 a.u., we observe that the increasing magnetic field boosts the energy of the singlet state $^1\Sigma_g$, and its potential curve rises highly above the curves of the triplet states. The potential well of the state $^3\Pi_u$ slowly deepens, and the location of its minimum shifts to smaller R. As a result, at $\gamma=1.0$ [Fig. 4(c)] the position of the potential minimum of the curve $^3\Sigma_u$ is very close to the point of intersection between curves $^3\Sigma_u$ and $^3\Pi_u$.

Because the singlet state $^1\Sigma_g$ now has a considerably higher energy than the triplet states, we can exclude it from consideration and concentrate more closely on the behavior of triplet states. Figures 4(d)–4(f) show the potential curves of the states $^3\Sigma_u$ and $^3\Pi_u$ in magnetic fields $\gamma=1.2$, 1.6, and 2.0 a.u. We observe that the behavior of the state $^3\Pi_u$ is opposite to the behavior exhibited by the singlet state $^1\Sigma_g$ in Figs. 3(d)–3(f). Namely, the potential minimum of $^3\Pi_u$ becomes located at a smaller internuclear distance than the intersection between curves $^3\Sigma_u$ and $^3\Pi_u$. This effect is observable already at $\gamma=1.6$ a.u. and is clearly seen at $\gamma=2.0$ a.u.

As we see, for magnetic fields stronger than $\gamma>1.2$ a.u. the potential minimum of the state $^3\Pi_u$ lies below the potential curve of the state $^3\Sigma_u$. This means that the triplet state $^3\Pi_u$, which is unstable in weaker fields, is now able to form metastable molecules. If two hydrogen atoms form a strongly bound molecule in the state $^3\Pi_u$ with internuclear distance close to the equilibrium position, they will remain in this state until the nuclei separate into a distance sufficiently large to allow a transition to the ground state $^3\Sigma_u$. The lifetime of such molecules will be determined mainly by the frequency and amplitude of their vibrational and rotational oscillations. Investigation of this question requires a detailed study of the potential energy surfaces of both triplet states and is a very interesting yet computationally difficult task for future research in this area. As for now, our results allow us to make a preliminary conclusion that the formation of metastable molecules starts approximately from $\gamma\approx1.4$ a.u.

With the further growth of the magnetic field the depth of the potential well of the state $^3\Pi_u$ continues to increase, which facilitates the formation of the metastable molecules. Figures 5(a) and 5(b) show the potential curves of the states $^3\Sigma_u$ and $^3\Pi_u$ in magnetic fields $\gamma=5$ a.u. and $\gamma=10$ a.u.

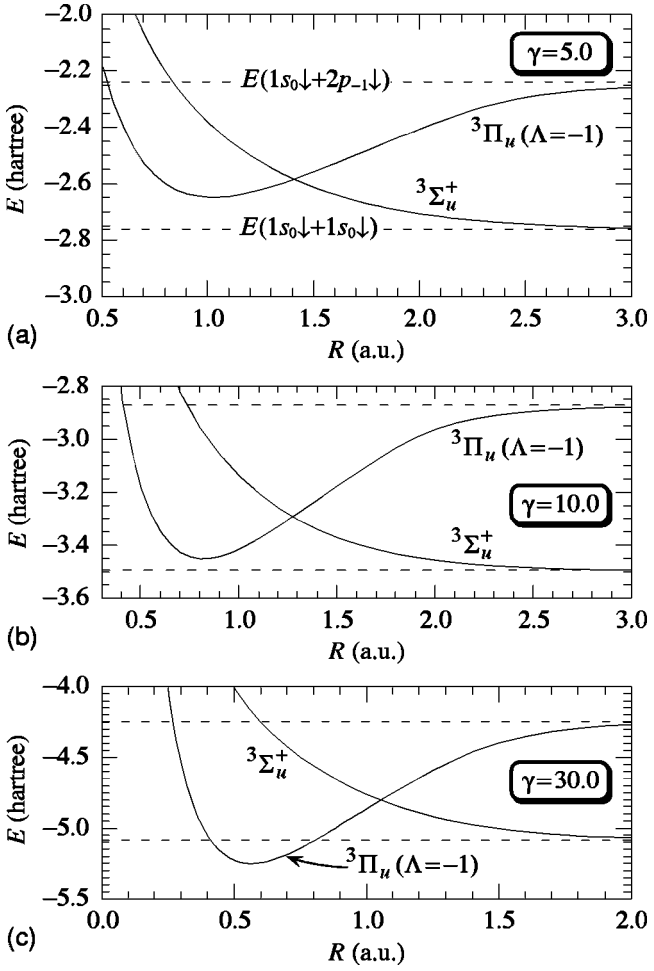

FIG. 5. Potential curves of the states $^3\Sigma_u$ and $^3\Pi_u$ in a parallel magnetic field (a) $\gamma=5$ a.u., (b) $\gamma=10$ a.u., and (c) $\gamma=30$ a.u.

Although the true ground state of the molecule is still the weakly interacting state $^3\Sigma_u$, the potential minimum of the state $^3\Pi_u$ gradually approaches the ground state energy. If the field increases to $\gamma=30$ a.u. [Fig. 5(c)], the potential well of $^3\Pi_u$ becomes sufficiently deep to make the strongly bound state $^3\Pi_u$ the ground state of the hydrogen molecule.

Therefore, the second transition of the ground state symmetry of H_2 happens at some magnetic field strength γ_2 such that $10<\gamma_2<30$ a.u. We have already seen that the first ground state transition from $^1\Sigma_g$ to $^3\Sigma_u$ happens at a certain γ_1 between 0.1 and 0.2 a.u. To determine the values of γ_1 and γ_2, we should turn to Fig. 6, which shows the dependence of the potential minima of all three state $^1\Sigma_g$, $^3\Sigma_u$, and $^3\Pi_u$ on the strength of the applied magnetic field in the region of weak and intermediate fields from $\gamma=0$ to 0.5 a.u. The solid lines show results calculated in the Hartree-Fock approximation; the dotted lines show the same potential curves corrected by the value of the correlation energy in the absence of a magnetic field. We have proved that for magnetic fields $0\leqslant\gamma\leqslant1$ a.u. the correlation energy remains almost constant, and so the dotted curves give a very accurate description of the actual behavior of potential minima with electron correlation taken into account. As we see, the first transition of the ground state symmetry from γ_1 to γ_2 happens at $\gamma_1\approx0.18$ a.u.

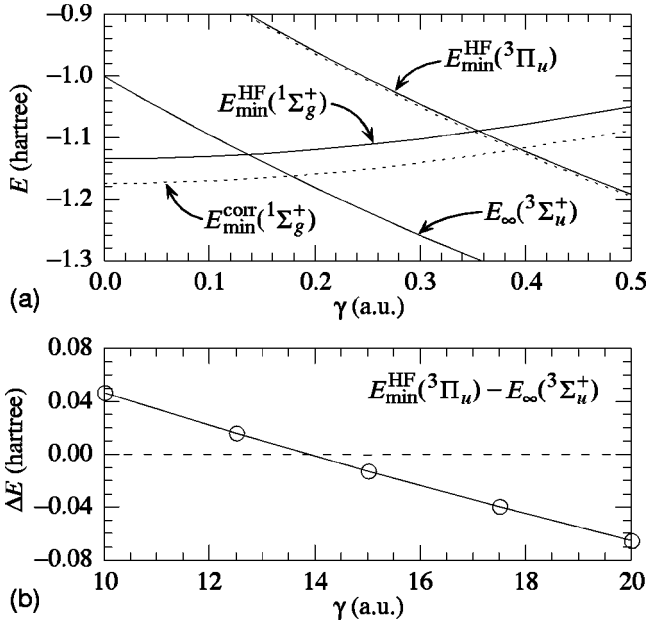

FIG. 6. Transitions of the ground state symmetry of the hydrogen molecule in a parallel magnetic field. (a) Energy minima of the states $^1\Sigma_g$, $^3\Sigma_u$, and $^3\Pi_u$ $(\Lambda=-1)$ as functions of the magnetic field strength γ. Solid curves show HF results; dotted curves show the correction for the electron correlation. (b) Difference between the potential minima of the states $^3\Pi_u$ and $^3\Sigma_u$.

Figure 6(b) shows the area of the second transition. Because of the absence of reliable data on the correlation energy in such magnetic fields, we are restricted to the Hartree-Fock (HF) approximation only. Figure 6(b) plots the difference between the HF energy of the potential minimum of the state $^3\Pi_u$ and the energy of two hydrogen atoms at infinite separation. The picture shows that the second transition of the ground state symmetry from $^3\Sigma_u$ to $^3\Pi_u$ occurs at $\gamma_2\approx14$ a.u.

Let us summarize our observations.

(1) For magnetic fields ranging from zero to $\gamma_1\approx0.18$ a.u., the ground state of the hydrogen molecule is the singlet state $^1\Sigma_g$.

(2) For magnetic fields ranging from γ_1 to $\gamma_2\approx14$ a.u., the ground state of the hydrogen molecule is the triplet state $^3\Sigma_u$ with a very weak interaction between atoms at large internuclear distances and with a repulsive potential at small and intermediate R.

(3) For magnetic fields ranging from γ_2 and stronger, the ground state of H_2 is the strongly bound triplet state $^3\Pi_u$. This result is probably valid for fields up to $\gamma=10^3$ a.u.; however, a correct description of the hydrogen molecule in magnetic fields stronger than $\sim10^3$ a.u. must take into account the effect of finite nuclear mass.

In addition to this general picture, there are two regions of magnetic field strength where the hydrogen molecule has strongly bound metastable states.

(1) If the magnetic field is in the range $\gamma_1<\gamma<\gamma_1^*\approx0.4$ a.u., the hydrogen molecule has a strongly bound metastable singlet state $^1\Sigma_g$. The ground state is $^3\Sigma_u$.

(2) If the magnetic field lies within the bounds $\gamma_2^*\approx1.4$ a.u.$<\gamma<\gamma_2$, the hydrogen molecule has a strongly bound metastable triplet state $^3\Pi_u$. The ground state is $^3\Sigma_u$.

The most important conclusion which follows from these results is that between γ_1 and γ_2 hydrogen in its ground state does not form strongly bound molecules. Instead, two atoms will form a molecule in the state $^3\Sigma_u$, and the pair interaction between hydrogen atoms is strongly repulsive at small internuclear distances and is very weak at large R. This means that hydrogen will form a gas of separated atoms with a weak anisotropic interaction due to the large quadrupole moments of the atoms.

VI. EXCITONIC SPECTRUM IN A MAGNETIC FIELD

As was already pointed out in the Introduction, the behavior of atomic hydrogen and of hydrogen molecules in a strong magnetic field is a subject of special interest because their close analogs, the hydrogenlike excitons and excitonic molecules, can be investigated in experiments with magnetic fields available in the laboratory. The experimental efforts are concentrated in two major directions. First, it is the investigation of highly excited states of excitons in semiconductors with large values of the effective critical magnetic field $H_0^{\rm eff}$. For a semiconductor such as Cu_2O the critical magnetic field is about 800 T, and laboratory magnetic fields of the order $10^{-2}H_0^{\rm eff}$ reveal the ''chaotic'' behavior of the excitonic spectrum [48]. The second direction of research is focused on the behavior of excitons in semiconductors with such effective critical magnetic fields that they may be reached in laboratory conditions. An example of such a material is uniaxially deformed germanium. This semiconductor is especially interesting because it does not restrict the experimenters to the study of separated excitons only but allows the investigation of excitonic molecules, or biexcitons as well [49].

Experiments with Ge in magnetic fields up to 14 T, which were reported recently [27], revealed interesting features of the excitonic spectrum. Reference [27] studied the optical spectrum of the uniaxially deformed germanium with the critical magnetic field $H_0^{\rm eff}=2.9$ T. The excitonic spectrum in the absence of a magnetic field consisted of two lines corresponding to excitons and to biexcitonic molecules. Application of the external magnetic field caused the decrease of intensity of the biexcitonic line and the final disappearance of this line at ≈ 1.5 T. This field strength corresponds to the effective magnetic field $\gamma \approx 0.5$ a.u. The further increase of the applied magnetic field to 4 T brought no significant qualitative changes in the spectrum. However, as the field reached 4 T ($\gamma \approx 1.4$ a.u.), an unknown spectral line emerged on the ''red'' side of the line of free excitons. It was labeled as the ''X line'' and associated with the appearance of another bound state, whose energy is by one e-h pair lower than the energy of an isolated exciton. The intensity of the X line grew with the increase of the magnetic field and at $H=10$ T ($\gamma \approx 3.5$ a.u.) constituted 15% of the intensity of the excitonic line.

The authors of [27] proposed two possible theoretical explanations of the observed spectrum. The first explanation, which the authors however doubted, was based on the assumption that the applied magnetic field increases the stability of the electron-hole liquid. The alternative explanation assumed the formation of a new biexcitonic molecular state. However, the nature of this state remained unclear due to the lack of information about the behavior of excitonic molecules in magnetic fields of intermediate strength $\gamma \sim 1$.

We suggest that the biexcitonic state which is responsible for the formation of the observed X line is the metastable triplet state $^3\Pi_u$. This claim is strongly supported by the fact that the strength of the magnetic field at which the X line appeared is in excellent agreement with the obtained value of γ_2^*. Further, the evolution of the X line with the growth of the magnetic field precisely corresponds to what one could expect from the metastable state $^3\Pi_u$: The stronger the magnetic field, the deeper the potential well of $^3\Pi_u$ and, therefore, the more metastable molecules can be formed, resulting in the increased intensity of the spectral line.

If this picture is valid, then spectral features similar to those observed in [27] for the case of germanium may be observed for other kinds of semiconductors as well. If other semiconductors with hydrogenlike excitons will exhibit the appearance of a similar X line at approximately the same effective strength of the applied magnetic field $\gamma \approx 1.4$ a.u., it will be a decisive argument in support of our hypothesis. Moreover, such an effect may open alternative possibilities for controlling the optical properties of semiconductors by using the externally applied magnetic field. Since the magnetic field required for such a control may be rather small (the critical magnetic field for InSb, for example, is $H_0^{\rm eff} \approx 0.2$ T), this mechanism may have potential technological applications. There is a clear and strong need for further experimental research in this area.

VII. CONCLUSIONS

We have investigated low-lying levels of the hydrogen molecule placed in a strong parallel magnetic field. The calculations were performed in the Hartree-Fock approximation using a fully numerical method. Effects of finite nuclear mass and corrections of higher order were neglected.

Most of our attention has been concentrated on the behavior of the hydrogen molecule in the intermediate region of the magnetic field strengths. We have followed the evolution of molecular levels in the magnetic field changing from $\gamma=0$ to 30 a.u. It is found that for a magnetic field in the range $0<\gamma<\gamma_1 \approx 0.18$ a.u. the ground state of the hydrogen molecule is the strongly bound singlet state $^1\Sigma_g$, for a magnetic field $\gamma_1<\gamma<\gamma_2 \approx 14$ a.u. the ground state of H_2 is the weakly interacting triplet state $^3\Sigma_u$, and for magnetic fields stronger than γ_2 the ground state of the molecule is the strongly bound triplet state $^3\Pi_u$. In addition to this general picture, there exist two regions of magnetic field strength, where the ground state of the molecule is the weakly interacting $^3\Sigma_u$, but hydrogen can form strongly bound metastable states. The first such region is $\gamma_1<\gamma<\gamma_1^* \approx 0.4$ a.u., where hydrogen may form metastable molecules in the singlet state $^1\Sigma_g$. The second metastable region lies within the bounds $\gamma_2^* \approx 1.4$ a.u.$<\gamma<\gamma_2$. For magnetic fields of such strength, hydrogen may form strongly bound metastable molecules in the state $^3\Pi_u$.

Since the ground state of H_2 for magnetic fields between γ_1 and γ_2 is the weakly interacting triplet state $^3\Sigma_u$, in this region of magnetic field strength hydrogen will behave like a nonideal Bose gas with a weak anisotropic interaction between atoms. This conclusion provides a solid foundation for

the theory of Bose condensation and superfluidity of a hydrogenlike gas in a strong magnetic field [33]. Although these effects must exist not for extremely strong magnetic fields but for magnetic fields less than 14 a.u., the principal concepts of [33] are proved to be valid.

Calculated results provide a possible theoretical explanation of the unusual features of the excitonic spectrum of germanium in a strong magnetic field, observed in [27]. The unknown excitonic ''X line'' observed experimentally may be ascribed to the formation of metastable biexcitons in the triplet state $^3\Pi_u$. We propose to perform new experiments with different kinds of semiconductors in strong magnetic fields. If the proposed explanation of the nature of the observed excitonic spectrum is confirmed, it may open new technological possibilities for controlling the optical properties of semiconductors.

ACKNOWLEDGMENTS

This work was supported in part by Swedish National Research Council (NFR) Contract No. F-AA/FU 10297-307, and in part by the Swedish Royal Academy of Sciences.

APPENDIX A: MOLECULAR INTEGRALS

The overlap integrals over spatial orbitals $S_{ab}=\langle u_a|u_b\rangle$ are given by

$$S_{ab}=\delta(m_a,m_b)\frac{\pi R^3}{4}\int_1^\infty d\xi\int_{-1}^1 d\eta(\xi^2-\eta^2)\phi_a\phi_b. \tag{A1}$$

The Hamiltonian integrals $H_{ab}=\langle u_a|\hat{h}|u_b\rangle$ are

$$\begin{aligned}H_{ab}=&-\delta(m_a,m_b)\frac{\pi R}{2}\int_1^\infty d\xi\int_{-1}^1 d\eta r_\perp^{|m_b|}e^{-\alpha/4\,\gamma r_\perp^2}\phi_a\\&\times\left[\hat{D}^{(\alpha\gamma)}_{|m_b|}f_b-\frac{1-\alpha^2}{16}\gamma^2R^2r_\perp^2(\xi^2-\eta^2)f_b\right.\\&\left.+(\mathcal{Z}_p\xi+\mathcal{Z}_m\eta)f_b\right]+\frac{\gamma}{2}(\alpha+|m_a|\alpha+m_b)S_{ab}.\end{aligned} \tag{A2}$$

The formulas for the Coulomb and exchange integrals g_{ab} at the positions of nuclei depend on the values m_a and m_b. The present work deals with combinations (0,0) and (0,−1), and the corresponding integrals are

$$g_{ab}\left(\begin{matrix}\mathbf{R}_1\\\mathbf{R}_2\end{matrix}\right)=\pi\int_1^\infty d\xi\int_{-1}^1 d\eta(\xi\mp\eta)K\phi_a\phi_b,$$

$$K=\begin{cases}\dfrac{R^2}{2}, & m_a=m_b=0,\\[2ex]\dfrac{r_\perp}{(\xi\pm\eta)^2}, & |m_a-m_b|=1,\ |\Lambda|=1.\end{cases} \tag{A3}$$

Here upper signs ''+'' and ''−'' should be taken for $\mathbf{R}_1$, and lower signs correspond to $\mathbf{R}_2$.

At large ξ potentials g_{ab} can be expressed via multipole series (since $G_{ab}=G^*_{ba}$, we may always assume that $m_a\geqslant m_b$),

$$\begin{aligned}g_{ab}(\xi,\eta)=&\frac{\pi R^2}{2}r_\perp^{-|m_b-m_a|}\sum_{l=m_a-m_b}^\infty\frac{(l-m_a+m_b)!}{(l+m_a-m_b)!}\\&\times(\xi^2+\eta^2-1)^{-(l+1)/2}\\&\times P_l^{m_a-m_b}\left(\frac{\xi\eta}{\sqrt{\xi^2+\eta^2-1}}\right)q_{ab}^{(l)},\end{aligned} \tag{A4}$$

where the moments $q_{ab}^{(l)}$ are defined by

$$\begin{aligned}q_{ab}^{(l)}=&\int_1^\infty d\xi\int_{-1}^1 d\eta,(\xi^2-\eta^2)(\xi^2+\eta^2-1)^{l/2}\\&\times P_l^{m_a-m_b}\left(\frac{\xi\eta}{\sqrt{\xi^2+\eta^2-1}}\right)\phi_a\phi_b.\end{aligned} \tag{A5}$$

It was sufficient to extend the summation over l in Eq. (A4) up to $l_{\max}=6$.

APPENDIX B: APPROXIMATION FORMULAS

The first and second derivatives are approximated by seven-point formulas (21). The coefficient matrices A and B are

$$A=\begin{pmatrix}-1&9&-45&0&45&-9&1\\2&-24&-35&80&-30&8&-1\\-10&-77&150&-100&50&-15&2\\-147&360&-450&400&-225&72&-10\end{pmatrix}, \tag{B1}$$

$$B=\begin{pmatrix}2&-27&270&-490&270&-27&2\\-13&228&-420&200&15&-12&2\\137&-147&-255&470&-285&93&-13\\812&-3132&5265&-5080&2970&-972&137\end{pmatrix}. \tag{B2}$$

For example, if we take the lower signs ''+'' and ''−'' in Eq. (21a) and put $k=2$, we obtain the following approximation for the first derivative:

$$\begin{aligned}y'(x_i)=&\frac{1}{60h}(-2y_{i-5}+15y_{i-4}-50y_{i-3}+100y_{i-2}\\&-150y_{i-1}+77y_i+10y_{i+1}).\end{aligned} \tag{B3}$$

[1] J. Trümper *et al.*, Ann. (N.Y.) Acad. Sci. **302**, 538 (1977); Astrophys. J. **219**, L105 (1978).
[2] J. C. Kemp, J. B. Swedlund, J. D. Landstreet, and J. R. P. Angel, Astrophys. J. **161**, L77 (1970).
[3] H. Friedrich and D. Wintgen, Phys. Rep. **183**, 37 (1989).
[4] X.-H. He, K. T. Taylor, and T. S. Monteiro, J. Phys. B **28**, 2621 (1995).
[5] G. Wunner, H. Ruder, and H. Herold, Phys. Lett. **79A**, 159 (1980).
[6] P. Schmelcher, L. S. Cederbaum, and H.-D. Meyer, J. Phys. B **21**, L445 (1988).
[7] D. Baye and M. Vincke, Phys. Rev. A **42**, 391 (1990).
[8] P. Schmelcher, L. S. Cederbaum, and U. Kappes, in *Conceptual Trends in Quantum Chemistry*, edited by E. S. Kryachko and J. L. Calais (Kluwer Academic Publishers, Dordrecht, 1994), pp. 1–51.
[9] Yu. P. Kravchenko, M. A. Liberman, and B. Johansson, Phys. Rev. A **54**, 287 (1996).
[10] Z. Chen and S. P. Goldman, Phys. Rev. A **48**, 1107 (1993).
[11] G. Fonte, P. Falsaperla, G. Schiffrer, and D. Stanzial, Phys. Rev. A **41**, 5807 (1990); P. Falsaperla and G. Fonte, *ibid.* **47**, 4143 (1993).
[12] A. Rutkowski and R. Kozlowski, J. Phys. B **30**, 1437 (1997).
[13] P. Pröschel *et al.*, J. Phys. B **15**, 1959 (1982); G. Thurner *et al.*, *ibid.* **26**, 4719 (1993).
[14] M. Vincke and D. Baye, J. Phys. B **22**, 2089 (1989).
[15] M.V. Ivanov, J. Phys. B **27**, 4513 (1994).
[16] D. M. Larsen, Phys. Rev. B **20**, 5217 (1979).
[17] C.-H. Park and A. F. Starace, Phys. Rev. A **29**, 442 (1984).
[18] D. Neuhauser, K. Langanke, and S. E. Koonin, Phys. Rev. A **33**, 2084 (1986); D. Neuhauser, S. E. Koonin, and K. Langanke, *ibid.* **36**, 4163 (1987).
[19] E. H. Lieb, J. P. Solovej, and J. Yngvason, Phys. Rev. Lett. **69**, 749 (1992); E. P. Lief and J. C. Weisheit, Contrib. Plasma Phys. **33**, 471 (1993); B. M. Relovsky and H. Ruder, Phys. Rev. A **53**, 4068 (1996).
[20] M. D. Jones, G. Ortiz, and D. M. Ceperley, Phys. Rev. A **54**, 219 (1996).
[21] M. Vincke and D. Baye, J. Phys. B **18**, 167 (1985).
[22] U. Kappes, P. Schmelcher, and T. Pacher, Phys. Rev. A **50**, 3775 (1994); U. Kappes and P. Schmelcher, *ibid.* **51**, 4542 (1995).
[23] Yu. P. Kravchenko and M. A. Liberman, Phys. Rev. A **55**, 2701 (1997).
[24] D. M. Larsen, Phys. Rev. A **25**, 1295 (1982).
[25] U. Wille, Phys. Rev. A **38**, 3210 (1988).
[26] U. Kappes and P. Schmelcher, Phys. Lett. A **210**, 409 (1996); Phys. Rev. A **53**, 3869 (1996).
[27] V. B. Timofeev and A. V. Chernenko, Pis'ma Zh. Eksp. Teor. Fiz. **61**, 603 (1995) [JETP Lett. **61**, 617 (1995)].
[28] A. V. Korolev and M. A. Liberman, Phys. Rev. A **45**, 1762 (1992); see also A. V. Korolev, Ph.D. thesis, Uppsala University, 1996, pp. 7–17.
[29] D. Lai, E. E. Salpeter, and S. L. Shapiro, Phys. Rev. A **45**, 4832 (1992); D. Lai and E. E. Salpeter, *ibid.* **53**, 152 (1996).
[30] M. Demeur, P.-H. Heenen, and M. Godefroid, Phys. Rev. A **49**, 176 (1994).
[31] M. Žaucer and A. Ažman, Phys. Rev. A **18**, 1320 (1978).
[32] Yu. E. Lozovik and A. V. Klyuchnik, Phys. Lett. **66A**, 282 (1978).
[33] A. V. Korolev and M. A. Liberman, Physica A **193**, 347 (1993); Phys. Rev. B **47**, 14 318 (1993); Phys. Rev. Lett. **72**, 270 (1994); Phys. Rev. B **50**, 14 077 (1994); Int. J. Mod. Phys. B **10**, 729 (1996).
[34] G. Ortiz, M. D. Jones, and D. M. Ceperley, Phys. Rev. A **52**, R3405 (1995).
[35] K. Runge and J. R. Sabin, Int. J. Quantum Chem. **64**, 561 (1997).
[36] T. Detmer, P. Schmelcher, F. K. Diakonos, and L. S. Cederbaum, Phys. Rev. A **56**, 1825 (1997).
[37] Yu. P. Kravchenko and M. A. Liberman, Phys. Rev. A **56**, 1825 (1997).
[38] L. Laaksonen, P. Pyykkö, and D. Sundholm, Int. J. Quantum Chem. **23**, 309 (1983); **23**, 319 (1983).
[39] *Handbook of Mathematical Functions*, edited by M. Abramowitz and I. A. Stegun (Dover, New York, 1965).
[40] G. Dahlquist and Å. Björck, *Numerical Methods* (Prentice-Hall, Englewood Cliffs, NJ, 1974), Sec. 5.6.
[41] J. M. Peek, J. Chem. Phys. **43**, 3004 (1965).
[42] J. L. Gázquez and H. J. Silverstone, J. Chem. Phys. **67**, 1887 (1977).
[43] J. C. Le Guillou and J. Zinn-Justin, Ann. Phys. (N.Y.) **154**, 440 (1984).
[44] M. S. Kaschiev, S. I. Vinitsky, and F. R. Vukajlović, Phys. Rev. A **22**, 557 (1980).
[45] G. Wunner, H. Herold, and H. Ruder, Phys. Lett. **88A**, 344 (1982).
[46] Yu. P. Kravchenko and M. A. Liberman, Int. J. Quantum Chem. **64**, 513 (1997).
[47] W. Kolos and L. Wolniewicz, J. Chem. Phys. **43**, 2429 (1965); W. Kolos and J. Rychlweski, J. Mol. Spectrosc. **66**, 428 (1977).
[48] H. Matsumoto, K. Saito, M. Hasuo, S. Kono, and N. Nagasawa, Solid State Commun. **97**, 125 (1996); N. Nagasawa (private communication).
[49] V. D. Kulakovskii, I. V. Kukushkin, and V. B. Timofeev, Sov. Phys. JETP **54**, 366 (1981).